Reports on Progress in Physics

Nuclear charge distributions

To cite this article: R C Barrett 1974 *Rep. Prog. Phys.* **37** 1

View the article online for updates and enhancements.

Related content

- Nuclear Coulomb energies
S Shlomo
- Nuclear sizes and the optical model
D F Jackson
- The nuclear surface
G A Jones

Recent citations

- One-pion exchange current effects on magnetic form factor in the relativistic formalism
Cun Zhang *et al*
- Beyond-mean-field study of elastic and inelastic electron scattering off nuclei
J. M. Yao *et al*
- DWBA theory for elastic scattering of polarized electrons from heavy unpolarized nuclei
D H Jakubassa-Amundsen

IOP ebooks™

Bringing together innovative digital publishing with leading authors from the global scientific community.

Start exploring the collection–download the first chapter of every title for free.

This content was downloaded from IP address 131.215.248.181 on 21/07/2020 at 22:46

Nuclear charge distributions

R C BARRETT

University of Surrey, Guildford, Surrey, UK

Abstract

Different methods of obtaining information about nuclear charge distributions are reviewed and the nature of this information is discussed. The calculations involved in the analysis of electron scattering and electronic and muonic atom measurements are described with particular reference to the approximations made and the small corrections which must be taken into account. A number of calculations based on dynamical models of the nucleus are discussed and examples are given of the resulting densities. Results are given for selected nuclei and for certain groups of isotopes and isotones, and comparisons are made between phenomenological and theoretically derived densities.

This review was completed in December 1972.

Contents

1. Introduction

The first direct determination of nuclear charge radii came from the electron scattering measurements of Lyman *et al* (1951). This was many years after the suggestion (Guth 1934) that, for fast electrons, the finite size of the nuclear charge distribution would produce large deviations from the cross section (Mott 1929) for scattering from a point charge. Electron scattering techniques then improved very rapidly and their use in the study of charge distributions and other properties of nuclei has been reviewed by Hofstadter (1956, 1957), Elton (1961), Bishop (1965), de Forest and Walecka (1966), de Forest (1967) and Überall (1971).

Two years after the experiments of Lyman *et al*, Fitch and Rainwater (1953) measured the energies of muonic atom x rays, which provided another means of determining nuclear charge radii. The idea of stopping negative muons in matter to form atoms and using x ray energies to obtain nuclear size information had come from Wheeler (1947). The accuracy of experiments on muonic atoms (formerly called mu-mesic or mu-mesonic atoms) improved slowly at first and then very rapidly after about 1960. The methods and the theoretical interpretation of the results have been reviewed by Rainwater (1957), Stearns (1957), West (1958), Sens (1963), Wu (1966), Wu and Wilets (1969), Devons and Duerdoth (1969), Burhop (1969), Wu (1971), Kim (1971) and Scheck and Hüfner (1973).

A much older method exists for the determination of *differences* between the nuclear charge radii of different isotopes of an element. This comes from the measurement of the isotope shift of spectral lines in electronic (ie ordinary) atoms. A similar shift (called the isomer shift) gives the change in the charge radius when a long-lived nuclear state is excited. Measurements of isotope shifts in which there was a substantial nuclear size effect were carried out by Merton (1919) but it was only later that the importance of the size contribution was realized (Bohr 1922).† Detailed calculations of the size of the effect were first carried out by Rosenthal and Breit (1932). Measurements of unusually large isotope shifts in the rare-earth region led Brix and Kopfermann (1949) to predict the existence of large intrinsic deformations in this region. Reviews of the subject have been given by Foster (1951), Brix and Kopfermann (1958), Breit (1958), Wilets (1958), Kuhn (1969) and Stacey (1966).

We shall not concern ourselves here with techniques which are used to give information about nuclear matter (ie neutron plus proton) radii. Examples are the scattering of nucleons, α particles and pions and the measurement of x ray energies in π-mesonic and K-mesonic atoms. Nor will we describe methods based on the measurements of coulomb energy differences between isobaric analogue states or mirror nuclei and which depend on assumptions about the structure of the nucleus. Apart from the fact that it is necessary to make assumptions in the analysis, these techniques are not as accurate as the direct methods described above. They are very useful, nevertheless, because they provide means of obtaining neutron radii. A review of some of the methods of obtaining information on nuclear matter distributions is given in the following paper (Jackson 1974). In what follows we shall

† The idea was attributed by Bohr to Kramers. There have been some references in the literature to a paper in 1931 on the size effect by Pauli and Peierls. This paper does not seem to have been published and Professor Peierls has no knowledge of its existence.

occasionally use the term 'nuclear size' as a shorthand term for 'shape and size of the nuclear charge distribution'.

Most of this discussion will be devoted to the determination of the radial shape of the charge distribution of spherical nuclei, but we shall also consider the angular dependence of the shape of nuclei which are not spherical. One of our prime aims will be to try to discover precisely what properties of the charge distribution can be obtained from the experiments and to what extent previously published density distributions are *determined* by the measurements as opposed to being merely consistent with them.

The interaction between charged leptons (ie electrons and positrons and muons) and nucleons consists of an electromagnetic and a weak term, and the latter has a completely negligible effect in the experiments considered here. The interaction with the magnetic moments of nucleons is most easily observed in measurements of electron scattering at 180° and of the hyperfine splitting of certain atomic levels. These measurements will not be discussed here and we shall confine our attention to situations where the electrostatic force dominates, so that almost all the effect comes from lepton–proton interaction. (The interaction with the neutron is not negligible and a small correction must be made for this.) It will be necessary to make certain approximations in order to reduce the many-body lepton–nucleus–electromagnetic field problem to a one-body problem described by the Dirac equation. The difference between the energy or cross section which comes from the solution of exact equations and that given by the Dirac equation can be expressed as a sum of correction terms such as the recoil, radiative and dispersion (or nuclear polarization) corrections. These will be carefully examined in the following sections. In many cases these corrections can be calculated accurately or shown to be small, so that the problem does reduce to solving the Dirac equations. This is not as easy as it may seem at first sight: to solve the equation numerically for the motion of a lepton in a given spherically symmetric potential *is* easy (with present day computers) but the inverse problem of proceeding from energies and cross sections to the charge distribution is not. The extent to which it can be solved will occupy much of our attention in this paper.

We must also consider whether it is necessary to correct for the effect of atomic electrons on electron scattering or muonic atom experiments. In electron scattering the energies we shall discuss range from about 50 to 750 MeV and this is above the region in which appreciable deflections or energy losses are caused by collisions with the atomic electrons. The small correction due to the latter can be calculated and is called the Landau straggling correction. When a muonic atom is formed the captured muon is at first strongly influenced by the presence of the atomic electrons which shield it from the nucleus. As the muon loses energy it either excites the surrounding electrons or the nucleus, or it emits radiation. The latter alternative is the most probable when the radius of the muon orbit is less than that of a 1S electron and this occurs when the principal quantum number n of the muon reaches a value of about 14.† The only muon states in which we are interested here, ie those in which the nuclear size effect is appreciable ($n \leqslant 3$), are barely influenced by the screening due to the electrons. The effect of the latter can be calculated as a small correction. This means that for our purposes the muonic atom can be treated as a one-lepton system.

† For a hydrogen-like atom the muon orbits are smaller than electron orbits by a factor of 207, the muon–electron mass ratio.

2. Calculations for spherical nuclei

The motion of electrons or muons bound in atomic orbits is not very relativistic for low-Z atoms, whereas in electron scattering experiments capable of giving information about the size of the nucleus the electrons are extremely relativistic. Nevertheless, because of the great accuracy of atomic measurements, a relativistic theory must be used for both scattering and bound-state problems. Initially we assume that the motion of the electron or muon is described by the Dirac equation for leptons moving in a fixed external field (the average field of the nuclear charge distribution), ie that the nucleus is infinitely heavy and has no internal degrees of freedom. Afterwards we discuss corrections to this approximation.

2.1. Motion in a fixed spherically symmetric field

For a static field the Dirac equation is†

$$[-i\hbar c\boldsymbol{\alpha}.\nabla+\beta mc^2+V(\boldsymbol{r})-E]\psi(\boldsymbol{r})=0 \tag{2.1}$$

where β and each of the three components of $\boldsymbol{\alpha}$ form a set of constant 4×4 matrices (the Dirac matrices) and ψ is a 4-component column vector (or spinor). If the potential $V(\boldsymbol{r})$ is due to the electrostatic force between a charge distribution $Ze\rho(\boldsymbol{r})$ and the (negatively charged) lepton then

$$V(\boldsymbol{r})=-Ze^2\int\frac{\rho(\boldsymbol{r}')\,\mathrm{d}^3r'}{|\boldsymbol{r}-\boldsymbol{r}'|} \tag{2.2}$$

where the normalization of $\rho(\boldsymbol{r})$ is such that

$$\int\rho(\boldsymbol{r})\,\mathrm{d}^3r=1. \tag{2.3}$$

If $\rho(\boldsymbol{r})$ is spherically symmetric then the general solution to equation (2.1) can be expressed as a linear combination of terms, each of which is a solution to equation (2.1) corresponding to a particular value of the total angular momentum j and parity. For each such term the spinor ψ can then be written

$$\psi=\begin{pmatrix}\dfrac{G(r)}{r}\mathscr{Y}_{ljm}\\[2ex]\dfrac{\mathrm{i}F(r)}{r}\mathscr{Y}_{l'jm}\end{pmatrix}$$

where $\mathscr{Y}_{ljm}$ is a 2-component spinor obtained by coupling a spin angular momentum of magnitude $\frac{1}{2}$ to an orbital angular momentum of magnitude l to form a total angular momentum of magnitude j and z-component m. The parity of ψ is $(-1)^l$ and the value of l' is $l+1$ for $j=l+\frac{1}{2}$ and $l-1$ for $j=l-\frac{1}{2}$. Equation (2.1) reduces to a pair of coupled first order radial equations:

$$\hbar c\left(\frac{\mathrm{d}F}{\mathrm{d}r}-\frac{\kappa}{r}F\right)=-(E-mc^2-V)\,G \tag{2.4a}$$

$$\hbar c\left(\frac{\mathrm{d}G}{\mathrm{d}r}+\frac{\kappa}{r}G\right)=(E+mc^2-V)\,F. \tag{2.4b}$$

† See eg Dirac (1958), Sakurai (1967).

The functions $G(r)/r$ and $F(r)/r$ are respectively the 'large' and 'small' radial components of the wavefunction. The constant κ is an integer of magnitude $(j+\frac{1}{2})$ which is negative for $j = l+\frac{1}{2}$ and positive for $j = l-\frac{1}{2}$. Although the orbital angular momentum is not conserved, spectroscopic notation is frequently used, eg the symbols $S_{1/2}$, $P_{1/2}$, $P_{3/2}$, $D_{3/2}$ and $D_{5/2}$ correspond to the $\kappa = -1, 1, -2, 2$ and -3 states respectively. The orbital angular momentum denoted by the spectroscopic symbol is that of the large component of the wavefunction. In the non-relativistic limit the equation for $G(r)/r$ reduces to the radial Schrödinger equation.

2.2. *Electron elastic scattering cross sections*

The scattering of an electron by a fixed nucleus of charge Ze may be represented by the diagram in figure 1. This represents an electron of initial momentum $\boldsymbol{p}$,

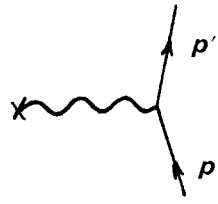

Figure 1. Electron scattering by a fixed nucleus.

final momentum $\boldsymbol{p}'$ which transfers momentum $\boldsymbol{q} = \boldsymbol{p} - \boldsymbol{p}'$ to the nucleus. For elastic scattering $|\boldsymbol{p}'| = |\boldsymbol{p}|$ and for a scattering angle θ, $|\boldsymbol{q}|$ is given by the equation†

$$q^2 = 4p^2 \sin^2 \tfrac{1}{2}\theta. \tag{2.5}$$

Equation (2.1) can easily be solved to first order in the potential, ie in the Born approximation which, for a point charge, leads to the 'Mott scattering formula' (Mott 1929).‡

$$\left(\frac{d\sigma}{d\Omega}\right)_M = \frac{4Z^2 e^4 E^2}{q^4 c^4}\left(1 - \frac{q^2 c^2}{4E^2}\right). \tag{2.6}$$

The effect of nuclear recoil may be taken into account by dividing the cross section by a factor§

$$1 + \frac{2E}{Mc^2}\sin^2 \tfrac{1}{2}\theta \tag{2.7}$$

where M is the mass of the nucleus. For high energies we can neglect the electron mass so that $E = pc$ and equation (2.6) becomes

$$\left(\frac{d\sigma}{d\Omega}\right)_M = \frac{Z^2 e^4}{4E^2}\frac{\cos^2 \tfrac{1}{2}\theta}{\sin^4 \tfrac{1}{2}\theta}. \tag{2.8}$$

† For a 3-vector $\boldsymbol{k}$ we use the symbol k to represent $|\boldsymbol{k}|$.

‡ The term 'Mott scattering' is sometimes used to refer simply to the scattering of relativistic electrons by a fixed point charge but the term 'Mott scattering formula' almost invariably means the approximate expression (2.6). Since cross sections are often expressed as a ratio to $(d\sigma/d\Omega)_M$ (given by 2.6) we sometimes find an exact theoretical cross section for an extended charge distribution expressed in terms of an approximate point-charge cross section.

§ See eg Hofstadter (1957).

In the non-relativistic limit the expression (2.6) reduces to the Rutherford scattering formula. For an extended nucleus the Born approximation for the non-relativistic scattering amplitude is proportional to

$$Ze^2 \int \rho(\boldsymbol{r}') \exp(\mathrm{i}\boldsymbol{q}.\boldsymbol{r}')\, \mathrm{d}^3r' \int \frac{\exp[\mathrm{i}\boldsymbol{q}.(\boldsymbol{r}-\boldsymbol{r}')]\, \mathrm{d}^3r}{|\boldsymbol{r}-\boldsymbol{r}'|} = \frac{Ze^2}{q^2} F(\boldsymbol{q})$$

where

$$F(\boldsymbol{q}) = \int \exp(\mathrm{i}\boldsymbol{q}.\boldsymbol{r})\, \rho(\boldsymbol{r})\, \mathrm{d}^3r. \tag{2.9}$$

The effect of the extended charge distribution is thus taken into account if the Rutherford cross section is multiplied by the factor $|F(\boldsymbol{q})|^2$. The same factor gives the relativistic cross section in the Born approximation in terms of the lowest order Mott scattering cross section

$$\left(\frac{\mathrm{d}\sigma}{\mathrm{d}\Omega}\right) = \left(\frac{\mathrm{d}\sigma}{\mathrm{d}\Omega}\right)_{\mathrm{M}} |F(\boldsymbol{q})|^2. \tag{2.10}$$

If $\rho(\boldsymbol{r})$ is spherically symmetric then $F(\boldsymbol{q})$ is a function of q^2 only:

$$F(\boldsymbol{q}) = \frac{4\pi}{q} \int_0^\infty r \sin(qr)\, \rho(r)\, \mathrm{d}r \tag{2.11}$$

$$= 1 - \frac{q^2\langle r^2\rangle}{3!} + \frac{q^4\langle r^4\rangle}{5!} - \ldots \tag{2.12}$$

where

$$\langle r^n\rangle = \int \rho(\boldsymbol{r})\, r^n\, \mathrm{d}^3r \tag{2.13}$$

is the mean nth power moment (or nth power radius) of the charge distribution.

The condition for validity of the Born approximation is

$$\frac{Ze^2}{\hbar v} \ll 1 \tag{2.14}$$

which in the relativistic limit becomes

$$\frac{Ze^2}{\hbar c} = Z\alpha \ll 1 \tag{2.15}$$

where $\alpha \simeq 1/137$ is the fine structure constant. Part of the effect of higher order contributions to the cross section may be taken into account by using an effective momentum transfer q' given by (Downs *et al* 1957, de Forest and Walecka 1966)

$$q' = q(1 - V(0)/p)$$
$$= q(1 + 3Z\alpha/2pR)$$

where we obtain the second expression if we approximate the nuclear charge distribution by a uniform sphere of radius R. The expression for the second Born approximation has been given for point-charge scattering by McKinley and Feshbach (1948) and Dalitz (1951) and for an extended charge by Budini and Furlan (1959). The second Born approximation amplitude is actually infinite but the contribution to the cross section is finite. It is instructive to write down the

integral which gives the second order contribution to the amplitude

$$f_2(\boldsymbol{p}, \boldsymbol{p}') \propto \int \mathrm{d}^3k \frac{F(\boldsymbol{p}'-\boldsymbol{k})}{|\boldsymbol{p}'-\boldsymbol{k}|^2} \langle k| G_0 |k\rangle \frac{F(\boldsymbol{k}-\boldsymbol{p})}{|\boldsymbol{k}-\boldsymbol{p}|^2} \tag{2.16}$$

where $\langle k| G_0 |k\rangle$ is the free electron propagator. Without evaluating this integral we can see how the interpretation of experimental cross sections becomes more difficult when second or higher order terms are not negligible and we can no longer extract the form factor from the data. One test of the validity of the first Born approximation is to check whether the ratio of the experimental to Mott cross section is independent of energy for a fixed q^2.

For cases in which the inequality (2.15) is not satisfied it is customary nowadays to do a phase shift analysis and solve the Dirac equation numerically. This was first done for an extended charge distribution by Elton (1950) and a detailed description of the method has been given by Yennie *et al* (1954). The equations (2.4) can be solved using a step-by-step method which integrates from the origin to the region of zero nuclear charge. This must be done for all κ values for which the wavefunction in the region of the nucleus is not negligible. The procedure is similar to that used for scattering of non-relativistic particles described by Jackson (1974). The scattering amplitude, and hence the cross section, can be obtained by comparing the numerical solutions with the known point-charge solutions to obtain phase shifts. A practical difficulty which complicates the calculation for high energy scattering is that much higher accuracy is required in the numerical integrations than that which is being sought in the cross sections. This is due to the almost complete cancellation in the scattering amplitude of contributions coming from different partial waves (ie different κ values). For example an accuracy better than one part per million in the phase shifts is necessary to achieve an accuracy of 1% in the cross section for 500 MeV scattering.

2.3. Radiation and straggling corrections in electron scattering

Important corrections to cross sections obtained by solving the Dirac equation are those due to the emission of real photons and the emission and reabsorption of virtual photons by the electron (Schwinger 1949) These processes can be represented by the diagrams in figure 2. Although the emission of a real photon means

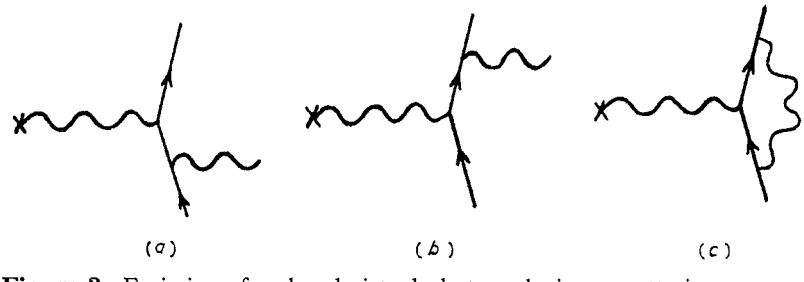

Figure 2. Emission of real and virtual photons during a scattering process.

that the scattering is not elastic, we must consider the emission of very soft photons, ie those whose total energy is less than the resolution of the electron detector (so that the electrons are counted as being elastically scattered). If we take into account only the process represented by figure 2(*c*), we get an infinite correction, but the

sum of the three terms is finite. The correction factor can be written in the form (Maximon 1969, Mo and Tsai 1969)

$$\left(\frac{d\sigma}{d\Omega}\right)_{corr} = \left(\frac{d\sigma}{d\Omega}\right)_{uncorr} e^{-\delta_1}(1-\delta_2) \tag{2.17}$$

where δ_1 and δ_2 are functions of the electron energy, scattering angle and the energy resolution, ΔE, of the detector.

$$\delta_1 = \frac{2\alpha}{\pi}\left(\ln\frac{q^2}{m^2c^2}-1\right)\ln\frac{\Delta E}{E} \tag{2.18}$$

$$\delta_2 = -\frac{2\alpha}{\pi}\frac{13}{12}\left(\ln\frac{q^2}{m^2c^2}-1\right)+\frac{17}{36}+\frac{\pi^2}{12}-\frac{L_2(\cos^2\frac{1}{2}\theta)}{2} \tag{2.19}$$

where

$$L_2(x) = -\int_0^x \frac{\ln(1-t)}{t}\,dt. \tag{2.20}$$

Since δ_1 can be large, the exponential factor in equation (2.17) cannot in general be replaced by the factor $(1-\delta_1)$ as was done in early calculations.

Another effect which produces a similar sort of correction to the cross section is multiple small-angle scattering by target nuclei which results in a straggling correction factor (Mo and Tsai 1969)

$$1 - bt\ln\frac{E}{\Delta E} \tag{2.21}$$

where b depends on the atomic number Z and t is the target thickness. This effect can be much larger than the Landau straggling which is due to multiple small-angle scattering by the atomic electrons and which can be neglected for our purposes (Landau 1944).

There are many other processes in which photons are emitted and reabsorbed or virtual electron positron pairs are created and then destroyed. Some of these are described in § 2.6 but they can be ignored for electron scattering.

2.4. Dispersion corrections in electron scattering

We now consider corrections to the approximation that the electron–nucleus interaction can be replaced by an electrostatic one-body potential $V(r)$. The hamiltonian for the electron–nucleus interactions may be written

$$H = H_0 + \delta H \tag{2.22}$$

where

$$H_0 = H_{free} + V(r) + H_N(\boldsymbol{r}_1, \boldsymbol{r}_2, \ldots, \boldsymbol{r}_A) \tag{2.23}$$

and

$$\delta H = -e^2\sum_{i=1}^{A} v(|\boldsymbol{r}_i - \boldsymbol{r}|) - V(r) \tag{2.24}$$

where $v(|\boldsymbol{r}_i - \boldsymbol{r}|)$ is the interaction between the electron and the ith nucleon. In equation (2.23) H_{free} is the hamiltonian for the free electron and $H_N(r_1, r_2, \ldots, r_A)$ is the hamiltonian for the nucleus in isolation. The term $V(r)$ is an arbitrary function of the electron coordinates and we choose it in such a way that if the

nucleus remains in its ground state, δH makes no first order contribution to the elastic scattering amplitude. This means that

$$\int \phi_N^* \, \delta H \, \phi_N \, d^3r_1 \, d^3r_2 \ldots d^3r_A = 0 \tag{2.25}$$

ie

$$V(r) = -e^2 \int \phi_N^* \sum_{i=1}^{A} v(|\boldsymbol{r}_i - \boldsymbol{r}|) \, \phi_N \, d^3r_1 \, d^3r_2 \ldots d^3r_A \tag{2.26}$$

where ϕ_N is the wavefunction for the ground state of the nucleus. Some of the higher order terms in δH which affect the elastic cross section can be obtained

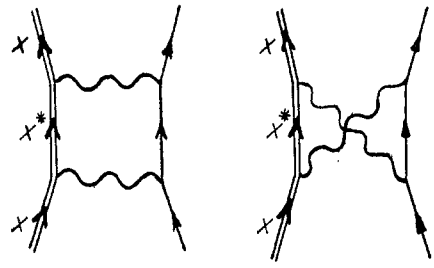

Figure 3. Second order dispersion terms.

from inelastic cross sections by making reasonable assumptions (de Forest and Walecka 1966), but in the absence of complete knowledge of the inelastic processes they are usually estimated on the basis of a simplified model of the nucleus. (There are also dispersion terms due to excitation of the nucleus by magnetic interactions which we have not included in δH.) The second order term may be represented by the diagram in figure 3 which shows a nucleus X being excited to an intermediate state X^* and then de-excited. Estimates have been made of the effect of the monopole part of δH (Rawitscher 1966, 1967, 1970) and the dipole part (Onley 1968). Rawitscher solved the coupled Dirac equations in the adiabatic approximation (ie neglecting nuclear excitation energies) and did a calculation only to second order in δH but to all orders in $V(r)$ (ie a second order distorted wave Born approximation calculation). Lin (1972) has calculated the corrections for ^{40}Ca using a single-particle model wavefunction for the ground state and plane waves for the intermediate states. Using a similar model Toepffer and Drechsel (1970) have obtained an imaginary part to be added to the electron–nucleus potential. Friar and Rosen (1972) have calculated the dispersion and other corrections for ^{12}C and ^{16}O using harmonic oscillator wavefunctions for the nuclear states. Three different methods have been used by Bethe and Molinari (1971) to calculate the corrections. All these estimates indicate that the errors caused in the determination of charge distributions by neglect of dispersion corrections are usually small, although the case of low energy scattering from Nd isotopes may be an exception (Rawitscher 1970) if the measurements of Madsen *et al* (1971) are not in error. (The skin thicknesses obtained in the analysis of these cross sections were anomalously small.)

2.5. Muonic atom energy levels

The energy eigenvalues of the Dirac equation (2.1) can be written in closed form for a point nucleus in terms of the muon mass m, the atomic number Z and the

fine structure constant $\alpha = e^2/\hbar c = [137{\cdot}036\,02(21)]^{-1}$ (Taylor *et al* 1969):

$$E = \frac{mc^2}{[1+(Z\alpha/n)^2]^{1/2}} \tag{2.27}$$

where

$$n = n' + [(j+\tfrac{1}{2})^2 - Z^2\alpha^2]^{1/2}. \tag{2.28}$$

Here n' is a non-negative integer and n becomes the principal quantum number in the non-relativistic limit ($Z\alpha \ll 1$). The expression (2.27) must be corrected for the effect of nuclear recoil but this can be done adequately by using the reduced mass in place of m (see Grotch and Yennie 1969). For the lowest states the extended nuclear charge produces corrections in the binding energy of up to 50% so that the size effect must be calculated exactly. For states in which the size effect vanishes there still remains an important correction to the expression (2.27) called the vacuum polarization correction. This is due to the presence of virtual electron–positron pairs which modify the potential at distances of the order of the reduced Compton wavelength of the electron ($\lambda\!\!\!^{-}_e = \lambda_e/2\pi = 386$ fm). It is discussed in § 2.6. The effect of both of these departures from the coulomb $(1/r)$ potential can be accounted for by solving the Dirac equation numerically for each muonic state of interest. For the lowest states this must be done for each shape and size assumed for the nuclear charge distribution. It is advantageous to use variable steps in r (eg equal steps in $\ln r$) in solving the equations so that they can be integrated out to values of r where the wavefunction becomes negligible. It is then possible to incorporate the correction due to vacuum polarization into the potential appearing in the Dirac equation and thus automatically include some of the higher order corrections.

2.6. Radiative and recoil corrections in muonic atoms

When we use the Dirac equation, we are solving a one-body problem. A more accurate procedure is to treat the lepton and nucleus as a two-body system and solve the Bethe–Salpeter equation. The recoil corrections to the Dirac equation energies can be expressed as a power series in the muon–nucleus mass ratio m/M. The first order correction is the same as the non-relativistic reduced mass correction and may be accounted for by substituting the reduced mass into the Dirac equation. The second order correction has been given for a point nucleus by Bethe and Salpeter (1967). For an extended nucleus the correction is (Barrett *et al* 1973)

$$\Delta E = -\frac{B^2}{2Mc^2} - \frac{B}{Mc^2} R\frac{\partial B}{\partial R} - \langle V_G \rangle \tag{2.29a}$$

where

$$V_G = \left(V^2 + \frac{2}{r^2}\frac{dV}{dr}\int_0^r r'^2\, V(r')\,dr'\right) \Big/ 2Mc^2 \tag{2.29b}$$

R is the equivalent radius (see appendix 1) and B is the muon binding energy. This results can be derived from the effective potential model of Grotch and Yennie (1969). This correction is smaller than experimental errors in those transitions in which it is not swamped by uncertainties in the nuclear polarization correction discussed in § 2.7.

It is more difficult to take account of the vacuum polarization and self-energy diagrams. The lowest order corrections are represented by the diagrams in figure 4 where we follow the usual convention of defining the order of a correction as the number of powers of e in the process (number of vertices) minus two (the number in the lowest order interation). Unlike the electronic atom case the most important correction in muonic atoms comes from vacuum polarization due to electron–positron pairs. (The vacuum polarization correction is sometimes called the *photon*

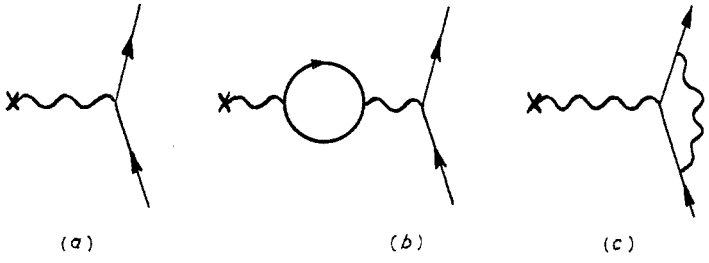

Figure 4. (*a*) Lowest order interaction, (*b*) second order vacuum polarization and (*c*) second order self-energy correction.†

self-energy correction.) This produces an additional potential $V_{\rm vp}(\boldsymbol{r})$ which is given by (see eg Akhiezer and Berestetskii 1965)

$$V_{\rm vp}(r) = -\frac{2}{3}Z\alpha^2\frac{\hbar c}{\pi}\int \rho(\boldsymbol{r}')\frac{K(|\boldsymbol{r}-\boldsymbol{r}'|)}{|\boldsymbol{r}-\boldsymbol{r}'|}\,\mathrm{d}^3r' \tag{2.30}$$

where

$$K(r) = \int_1^\infty \exp(-2yr/\lambda_{\rm e})\left(1+\frac{1}{2y^2}\right)(y^2-1)^{1/2}\frac{1}{y^2}\,\mathrm{d}y. \tag{2.31}$$

This integral can easily be evaluated numerically for each value of $|\boldsymbol{r}-\boldsymbol{r}'|$. It is necessary to evaluate $V_{\rm vp}(\boldsymbol{r})$ for every shape and size of the charge distribution $\rho(\boldsymbol{r}')$ being considered. There are a number of higher order vacuum polarization diagrams which must be taken into account in order to obtain agreement between theory and experiment for higher transitions (Dixit *et al* 1971) but in these cases the experiments do not provide any nuclear size information.

The self-energy correction in muonic atoms was neglected for many years but was found (Barrett *et al* 1967) to be much bigger than certain order-of-magnitude estimates. The correction is not large but for heavy nuclei it does have an effect on the nuclear size analysis. The correction corresponding to the lowest order diagram is given approximately (to first order in the field strength) by

$$\Delta E_n = \frac{\alpha}{3\pi m^2}\langle n|\nabla^2 V|n\rangle\left(\ln\frac{m}{2\Delta\epsilon}+\frac{11}{24}+\frac{3}{8}-\frac{1}{5}\right)+\frac{\alpha}{8\pi m^2}\left\langle n\left|\frac{2}{r}\frac{\partial V}{\partial r}\boldsymbol{\sigma}.\boldsymbol{L}\right|n\right\rangle. \tag{2.32}$$

The term $(-\frac{1}{5})$ takes account of vacuum polarization due to $\mu^+\mu^-$ pairs and the

† The self-energy correction is frequently called the Lamb shift and it is the dominant cause of the $2S_{1/2}$–$2P_{1/2}$ splitting in the (electronic) hydrogen atom (Lamb and Retherford 1947). The term 'Lamb shift' is sometimes used, however, to denote the whole of the $2S_{1/2}$–$2P_{1/2}$ splitting which is due to vacuum polarization and proton size effects as well as the electron self-energy term.

spin dependent term is the correction due to the anomalous magnetic moment of the muon. The 'Bethe logarithm' $\ln \Delta\epsilon$ is defined by the equation

$$\ln \frac{m}{2\Delta\epsilon} = \frac{\sum_{n' \neq n} \langle n | \boldsymbol{p} | n' \rangle \langle n' | [V, \boldsymbol{p}] | n \rangle \ln \dfrac{m}{2|E_n - E_{n'}|}}{\frac{1}{2} \langle n | \nabla^2 V | n \rangle}. \tag{2.33}$$

Barrett *et al* made the approximation of replacing $\Delta\epsilon$ by the binding energy of the muon in the state $|n\rangle$. For the particular case in which $|n\rangle$ is the ground state an accurate method of estimating $\Delta\epsilon$ has shown that it is in fact very close to the muon binding energy (Barrett 1968). For the lowest muon states the errors in the self-energy correction, together with the errors in the nuclear polarization correction, make the greatest contribution to the theoretical uncertainties in the energy levels.

2.7. Nuclear polarization corrections in muonic atoms

If we use a static potential to describe the muon–nucleus interaction in a muonic atom, the corrections to this approximation are very similar to the dispersion corrections to electron scattering described in § 2.4, and equations (2.22) to (2.26) may be applied to the muon case. Thus the choice (2.26) for $V(r)$ means that the energy correction to first order in δH is zero. The second order correction to the energy of a particular state results from the admixture of other muon states and nuclear excited states. Many authors have estimated the second order correction and detailed calculations have been carried out by Cole (1969), Chen (1968, 1970a) and Skardhamar (1970). We expand δH as a multipole series

$$\delta H = \sum_L \delta H_L \tag{2.34}$$

where, for $L = 0$,

$$\delta H_0 = -e^2 \sum_{i=1}^{Z} \frac{1}{r_>} - V(r) \tag{2.35}$$

and, for $L > 0$,

$$\delta H_L = -e^2 \sum_{i=1}^{Z} \frac{r_<^L}{r_>^{L+1}} P_L(\cos \theta_{i\mu}). \tag{2.36}$$

The second order correction to the state $|\mu I\rangle$ is given by

$$\Delta E_L = \sum_{\mu' I'} \frac{\langle \mu I | \delta H_L | \mu' I' \rangle \langle \mu' I' | \delta H_L | \mu I \rangle}{E_I + E_\mu - E_{I'} - E_{\mu'}}. \tag{2.37}$$

Although we need complete knowledge of the nuclear spectrum to evaluate the correction terms it turns out that for $L \geqslant 2$ the results are insensitive to the nuclear energies while for $L = 1$ they depend on the known energy of the giant dipole state. The greatest uncertainty arises from the $L = 0$ contribution which depends on the excitation energy of unobserved monopole excitations ('breathing modes') of the nucleus. These points are described in detail by Chen (1970a) and summarized by Wu and Wilets (1969). The uncertainties in the polarization corrections put a limit to the accuracy to which we can obtain information from muonic atoms about the size of the nuclear charge distribution.

2.8. Isotope and isomer shifts in electronic atoms

The energy corresponding to an atomic transition is slightly dependent on the mass and size of the nucleus and the difference between the energies for two different isotopes is called the isotope shift.† It is sometimes possible to measure the energy of an atomic transition which takes place where the nucleus is in a long-lived (isomeric) state and the resulting difference in energy between the ground state and the isomeric state transitions is called the isomer shift. In order to obtain information about the difference in charge distribution between different isotopes it is necessary to separate the contributions due to the change in mass (the 'mass shift') and to the change in the electric field (the 'field shift') which results from a nuclear size change. In many cases this can be done only approximately. There is no such difficulty, of course, in interpreting the isomer shift which is entirely a field effect. A discussion of recent progress in estimating the mass shift is given in § 2.8.2.

2.8.1. The field shift. The field shift is significant only if the transition involves a significant change in the overlap of the atomic wavefunction with the nucleus and this means a change in the configuration of $j = \frac{1}{2}$ states. If the modulus squared of the wavefunction for the $j = \frac{1}{2}$ electron is expressed as a power series in r^2:

$$|\psi(r)|^2 = \sum_{n=0}^{\infty} a_n r^{2n} \tag{2.38}$$

then the electrostatic potential $V_e(r)$ due to the electron is given by

$$V_e(r) = -e \sum_{n=0}^{\infty} b_n r^{2n} \tag{2.39}$$

where the coefficients b_n are given by

$$b_{n+1} = \frac{a_n}{(2n+2)(2n+3)}. \tag{2.40}$$

(We do not need b_0.) If we know $V_e(r)$ we can calculate the field shift to sufficient accuracy in first order perturbation theory,

$$\Delta E_{\text{field}} = C_1 \delta\langle r^2\rangle + C_2 \delta\langle r^4\rangle + C_3 \delta\langle r^6\rangle + \ldots \tag{2.41}$$

where

$$C_n = -Zeb_n. \tag{2.42}$$

The coefficients C_1, C_2 and C_3 have been tabulated for the 1S state for all values of Z in the range 30 to 103 by Seltzer (1969) who also tabulates C_1 for the 2S, $2P_{1/2}$ and 3S states. Seltzer points out that the ratio C_2/C_1 for a given nucleus is almost the same for the different $j = \frac{1}{2}$ states (implying that K x ray and optical shifts measure the same property of the nuclear charge). Most analyses of isotope shifts have used only the first term in the expression (2.41).

$$\Delta E_{\text{field}} \simeq C_1 \delta\langle r^2\rangle. \tag{2.43}$$

It is interesting to note that expression (2.43) was first derived using non-relativistic point-charge wavefunctions but later replaced by the 'more sophisticated' result based on relativistic point-charge wavefunctions which gave

$$\Delta E_{\text{field}} \simeq C_1' \delta\langle r^{2\sigma}\rangle \tag{2.44}$$

where

$$\sigma = (1 - Z^2\alpha^2)^{1/2}. \tag{2.45}$$

† For a more comprehensive review of isotope shifts see Stacey (1966).

The use of realistic (extended charge) relativistic wavefunctions essentially takes us back to the expression (2.43) (Bodmer 1953, 1959) and this means that expression (2.44) is incorrect.

Since we do not know how to separate the different contributions to δE_{field} in expression (2.41) any conclusions about the change in $\langle r^2 \rangle$ will depend somewhat on assumptions about the charge distribution. If we sum the series, we can say something more definite about the change in the charge distribution without such assumptions. This has been done by Wu and Wilets (1969) using the formula of Ford and Wills (1969). The result can be expressed in terms of a single fractional moment $\langle r^k \rangle$ of the charge distribution (see § 6.2). The values of k have been calculated by Ford (1972) and are shown in table 1. They can be obtained

Table 1. Values of C_1, C_2, C_3 and k for the 1S state. The units for C_n are meV fm^{-2n}

Z	C_1	C_2	C_3	k
30	6·83	−0·00232	$0{\cdot}95\times10^{-5}$	1·98
50	84·5	−0·0523	$0{\cdot}161\times10^{-3}$	1·95
60	238	−0·185	$0{\cdot}534\times10^{-3}$	1·93
70	623	−0·579	$1{\cdot}58\times10^{-3}$	1·91
82	1880	−2·11	$5{\cdot}59\times10^{-3}$	1·88
92	4700	−6·01	$15{\cdot}6\times10^{-3}$	1·85

fairly accurately from the expression

$$k = 2+\frac{4C_2R^2+12C_3R^4}{C_1+2C_2R^2+3C_3R^4} \tag{2.46}$$

where R is the approximate radius of the nuclear surface (or, more precisely, the 'average' radius of the function $r^2\Delta\rho$ where $\Delta\rho$ is the difference between the actual distribution and a uniform distribution).

2.8.2. The mass shift. The correction to the atomic energy levels due to the nuclear mass motion is given in the non-relativistic limit by the kinetic energy of the nucleus due to its motion about the centre of mass of the atom. This may be written as the sum of the two terms:†

$$\begin{aligned}\Delta E &= \frac{1}{2M}\left(\sum_i \boldsymbol{p}_i\right)^2 \\ &= \frac{1}{2M}\left(\sum_i \boldsymbol{p}_i^2+\sum_{i\neq j}\boldsymbol{p}_i\cdot\boldsymbol{p}_j\right)\end{aligned} \tag{2.47}$$

where M is the nuclear mass and $\boldsymbol{p}_i$ the momentum of the ith electron. Since the atomic wavefunctions are almost identical for different isotopes the expectation value of the expression in brackets is independent of M and the mass shift is thus proportional to the change in $1/M$:

$$\frac{\delta M}{M(M+\delta M)}.$$

The first term in (2.47) leads to the well-known reduced mass correction which results in the *normal mass shift* between isotopes. The evaluation of the second term, which gives rise to the *specific mass shift*, requires knowledge of the electron

† The presence of non-trivial mass terms was pointed out by Ehrenfest (1922) and a quantitative treatment was given by Hughes and Eckart (1930).

wavefunctions for excited states. Calculations of the specific mass shift are rare. A preliminary result of Bauche (1966) for the element Nd was in reasonable agreement with other methods of estimating the mass shift (Stacey 1971) but subsequent calculations (Bauche 1969) with better wavefunctions have given a much bigger result; it is difficult to estimate the error to be put on the theoretical calculations. For 2P–1S transitions estimates are probably more reliable and have been made by Chesler (1967) for Mo, Sn, Sm and W.

For large Z atoms the relativistic mass correction (2.29) becomes important and the ratio of the relativistic shift to the normal mass shift is $-Z^2\alpha^2/4$ for the 1S state, ie it varies from about 3% for Sn to 11% for U. Since this ratio is proportional to the square of the binding energy it is negligible for optical transitions.

2.8.3. King plots. Information about specific mass shifts can be obtained by plotting the shifts in one line for different pairs of isotopes against the corresponding shifts in other lines. This method is due to King (1963, 1964) and an example of such a plot is given in figure 5.

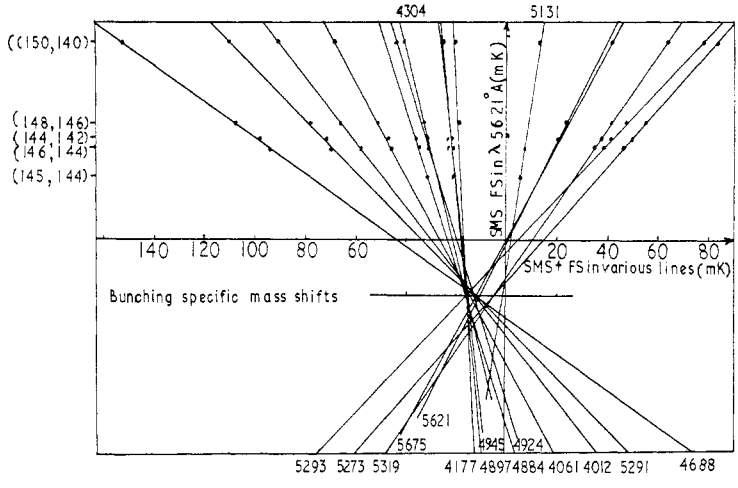

Figure 5. Field shifts plus specific mass shifts for Nd isotopes. The quantity $2\delta^i_{AA'}/144 \times 146$ (where i denotes the 5621 Å line) is plotted along the vertical axis and $2\delta^j_{AA'}/144 \times 146$ for various lines j along the horizontal axis.

The shift in line i between a pair of isotopes of mass number A and A' may be written

$$\begin{aligned}\delta E^i_{AA'} &= n^i_{AA'} + s^i_{AA'} + f^i_{AA'} \\ &= \frac{A'-A}{AA'} c^i_1 + \frac{A'-A}{AA'} c^i_2 + c^i_3 \, \delta\langle r^k \rangle_{AA'}\end{aligned} \tag{2.48}$$

where the terms on the right-hand side are the normal mass shift, specific mass shift and field shift respectively and the coefficients c^i_r to a very good approximation are independent of A and A'. We define a quantity

$$\begin{aligned}\delta^i_{AA'} &= \frac{AA'}{A'-A}(s^i_{AA'} + f^i_{AA'}) \\ &= c^i_2 + c^i_3 \frac{AA'}{A'-A} \delta\langle r^k \rangle_{AA'}\end{aligned} \tag{2.49}$$

which is derived from $\delta E^i_{AA'}$ after the known normal shift $n^i_{AA'}$ has been subtracted. A King plot is a graph of $\delta^j_{AA'}$ against $\delta^i_{AA'}$ for a number of different isotope pairs A, A' and for different spectroscopic lines i and j:

$$\delta^j_{AA'} = c^j_2 + \frac{c^j_3}{c^i_3}(\delta^i_{AA'} - c^i_2). \tag{2.50}$$

Any point on the line represents the values of the shifts which would be found in lines i and j for a particular value of $\delta\langle r^k\rangle$. One such point will correspond to $\delta\langle r^k\rangle = 0$ and at this point the two shifts will be equal to the respective specific mass shifts. If we plot the shifts for a number of transitions $\delta^l_{AA'}$, $\delta^m_{AA'}$ etc against $\delta^i_{AA'}$ for a set of isotopes then the specific mass shift for each line can be read off in terms of an assumed value of s^i. As can be seen in figure 5 the lines are bunched together at one point and King (1971) has argued that this is probably the point corresponding to zero field shift: if this is so, the specific mass shifts are determined. This method requires knowledge of isotope shifts for a large number of transitions and depends on the assumption that the mass shift does not depend in a systematic way on whether the initial or final state of the electron making a transition is an S state. Such a correlation could shift the region of bunching significantly and this question should be examined by direct calculations.

Another method, first suggested by Stacey (1966), is to plot the optical shifts against muonic x ray shifts which have no specific mass correction. Such plots were first made by Macagno (1968).† The method suffers from the disadvantage (Stacey 1971) that muonic and electronic energy levels depend on different properties of the charge distribution‡ and the error introduced by this is difficult to estimate.

3. Calculations for deformed nuclei

For some nuclei the lowest excitations are well described in terms of collective degrees of freedom (Bohr and Mottelson 1953) and it can be a bad approximation to ignore the effects of virtual nuclear excitations. For nuclei with large intrinsic deformations these effects can be taken into account by using a lepton–nucleus interaction potential $V(\boldsymbol{r}, \boldsymbol{\xi})$ which is not a spherically symmetric function of $\boldsymbol{r}$ and in which the coordinates $\boldsymbol{\xi}$ describe the orientation of the nucleus. The function $V(\boldsymbol{r}, \boldsymbol{\xi})$ can be derived from a non-spherical charge distribution $\rho(\boldsymbol{r}')$ where the prime indicates that $\boldsymbol{r}'$ is a position vector in a coordinate system fixed in the nucleus.§ We assume that $\rho(\boldsymbol{r}')$ has cylindrical symmetry (since for most nuclei this seems to give an adequate description of their properties) so that, after choosing

† See also Wu and Wilets (1969) and Macagno *et al* (1970). Note that when the normal mass shift is calculated for muonic atoms the effect due to the scaling of lengths as well as of energies must be taken into account. If we define $s = m\,\delta M/M(M+\delta M)$ then the normal mass shift is given to sufficient accuracy by the equation

$$(\delta E)_{\text{normal mass}} = sE_{\text{extended charge}} + ks(E_{\text{extended charge}} - E_{\text{point charge}})$$

where k is the Ford and Wills (1969) moment corresponding to the level being considered.

‡ See appendix 2.

§ This is not exactly equivalent to carrying out the correct procedure, namely, to use deformed intrinsic wavefunctions, projecting out the appropriate angular momentum eigenstate, and then using the exact lepton–nucleon potential $\sum_i v_i(\boldsymbol{r} - \boldsymbol{r}_i)$. The difference, however, is proportional to the square of the deformation parameter.

the z' axis along the symmetry axis, we can write

$$\rho(\boldsymbol{r}') = \sum_L \rho_L(r')\, P_L(\cos\theta') \tag{3.1}$$

The functions $\rho_L(r')$ are sometimes referred to as the 2^L-pole distributions or, explicitly, as the monopole, quadrupole, octupole and hexadecapole distributions for $L = 0, 2, 3, 4$ respectively. (For the appropriate choice of origin $\rho_L(r') \equiv 0$ for $L = 1$.)

3.1. Electron scattering by deformed nuclei

In Born approximation the scattering amplitude for a fixed deformed nucleus is proportional to

$$F(\boldsymbol{q}) = \int \exp(i\boldsymbol{q}.\boldsymbol{r})\, \rho(\boldsymbol{r})\, \mathrm{d}^3r \tag{3.2}$$

$$= \sum_L F_L(q^2)\, P_L(\theta') \tag{3.3}$$

where

$$F_L(q^2) \equiv \int j_L(qr)\, \rho_L(r)\, \mathrm{d}^3r \tag{3.4}$$

and θ' is the angle between $\boldsymbol{q}$ and the symmetry axis. For a spin 0 nucleus with intrinsic deformation the (spherically symmetric) ground state nuclear wavefunction is a linear superposition of deformed wavefunctions. We must thus average the scattering amplitude over angles θ' so that it becomes proportional to $F_0(q^2)$ and the cross section is proportional to the square of this quantity. Thus the effect of the deformation is completely taken into account by the effective radial shape $\rho_0(r)$.† Because of angular momentum selection rules this result is also true if the nucleus has spin $I = \frac{1}{2}$. If a nucleus has spin $I \geqslant 1$ and is polarized there is interference between the terms $F_L(q^2)$ in the amplitude. For unpolarized nuclei the interference terms vanish and the cross section for a nucleus with quadrupole deformation is given by

$$\frac{\mathrm{d}\sigma}{\mathrm{d}\Omega} \propto |F_0(q^2)|^2 + |F_2(q^2)|^2. \tag{3.5}$$

Inelastic scattering from $I = 0$ to $I = 2$ states is proportional to $|F_2(q^2)|^2$.

Where the Born approximation is inadequate we must solve the combined Dirac–Schrödinger equation for the electron–nucleus system:

$$(H_{\text{free}} + V(\boldsymbol{r}, \boldsymbol{\xi}) + H_{\text{N}}(\boldsymbol{\xi}) - E)\, \Psi = 0 \tag{3.6}$$

where H_{free} is the Dirac hamiltonian for a free electron and $H_{\text{N}}(\boldsymbol{\xi})$ is the kinetic energy operator for the nuclear rotational motion:

$$(H_{\text{N}}(\boldsymbol{\xi}) - \epsilon_I)\, \phi_{IM} = 0. \tag{3.7}$$

Expanding Ψ in eigenfunctions ϕ_{IM},

$$\Psi = \sum_{IM} \phi_{IM}\, \psi_{IM} \tag{3.8}$$

† Strictly speaking we should instead average the intrinsic wavefunction over angles and then square it to obtain $\rho_0(r)$. In practice the difference between the two methods is not significant.

we obtain coupled Dirac equations for the spinors ψ_{IM}:

$$[H_{\text{free}} + \langle IM \,|\, V \,|\, IM\rangle + \epsilon_{I'} - E]\psi_{I'M'} = -\sum_{IM \neq IM'} \langle I'M' \,|\, V \,|\, IM\rangle \psi_{IM}. \quad (3.9)$$

These equations can be reduced to coupled radial equations in functions $F^I_{n\kappa j}(r)$ and $G^I_{n\kappa j}(r)$ by the usual partial wave expansions. In practice they are usually solved approximately by substituting the solutions of the homogeneous equations on the right-hand side of equation (3.9) (the distorted wave Born approximation). Detailed descriptions of the theory of electron scattering from deformed nuclei have been given by de Forest and Walecka (1966) and Raphael and Rosen (1970).

3.2. Muonic atoms with deformed nuclei

In muonic atoms deformation of the nuclear charge distribution can cause hyperfine splitting just as it does in electronic atom spectra. Because of the small muon magnetic moment this effect dominates magnetic hyperfine splitting. Another important difference between the two kinds of atoms is the size of the effect: in muonic atoms second order terms are so large that the splitting can be observed in the spectra for spin 0 nuclei. Calculations of this 'dynamic hyperfine splitting' were first carried out by Wilets (1954) and by Jacobsohn (1954). A recent description of the method, together with experimental results for a number of nuclei, has been given by Hitlin *et al* (1970).

If we assume that the charge distribution has the form (3.1) then the potential can be expanded similarly

$$V(\boldsymbol{r}, \boldsymbol{\xi}) = \sum_L V_L(r') P_L(\cos\theta') = \sum_{LM} V_L(r) Y_{LM}(\theta, \phi)\, Y^*_{LM}(\hat{\boldsymbol{\xi}}) \quad (3.10)$$

where the angles $\hat{\boldsymbol{\xi}}$ give the orientation of the symmetry axis. For large distances the term $V_2(r)$ becomes

$$V_2(r) \xrightarrow[r\to\infty]{} -\frac{e^2 Q_0}{2r^3}$$

where Q_0 is the intrinsic quadrupole moment of the nucleus. The energy levels of the muonic atom may be found by constructing a basis of states $|IKn\kappa j;\, FM\rangle$ from nuclear states $|IKM\rangle$ and muon states $|n\kappa j\rangle$ which are eigenstates of the hamiltonian $[H_{\text{free}} + V_0(r)]$. In practice only muon states of the same principal quantum number n are strongly mixed,† so that we can construct a 'model space' of states with the same value of n and diagonalize the restricted matrix of the hamiltonian. The effect of the mixing of other states may then be taken into account by second order perturbation theory (Chen 1970b). As an example let us consider the splitting in the muon 2P state for a quadrupole deformation and restrict the nuclear states to $I = 0$ and $I = 2$. The resulting model space consists of the states shown in table 2.

Table 2. Possible states of angular momentum F from nuclear states $I = 0, 2$ and muon states $j = \frac{1}{2}, \frac{3}{2}$

I	0	2		0	2	2		2	2	2
j	$\frac{1}{2}$	$\frac{3}{2}$		$\frac{3}{2}$	$\frac{1}{2}$	$\frac{3}{2}$		$\frac{1}{2}$	$\frac{3}{2}$	$\frac{3}{2}$
F	$\frac{1}{2}$	$\frac{1}{2}$		$\frac{3}{2}$	$\frac{3}{2}$	$\frac{3}{2}$		$\frac{5}{2}$	$\frac{5}{2}$	$\frac{7}{2}$

† This happens when the nuclear first excited state has an energy of the order of the fine structure splitting, eg in ^{182}W they are 100 keV and 150 keV respectively. The off-diagonal matrix elements of H are of the order of 50 keV.

The eight energy levels obtained by diagonalizing the hamiltonian matrix depend on the magnitude and sign of the diagonal and off-diagonal elements of the quadrupole operator between nuclear states. In practice only three of the levels have been observed (since the intensity of transitions to the others is very low) so that we cannot separately determine these quantities yet.

The second order corrections to the energies obtained from the restricted model space can be taken into account by using a renormalized or effective interaction V inside the model space. This method has been described by Chen (1970b) who finds that it gives good agreement with a coupled channels Dirac equation calculation of McKinley (1969).

4. Direct calculations of nuclear charge distributions from nuclear theory

For a nucleus with a ground state $\Phi(\boldsymbol{r}_1, \boldsymbol{r}_2, \ldots, \boldsymbol{r}_A)$ the probability densities $Z\rho_p(\boldsymbol{r})$ for protons and $N\rho_n(\boldsymbol{r})$ for neutrons are given by

$$Z\rho_p(\boldsymbol{r}) = \int \Phi^* \sum_{i=1}^{Z} \delta(\boldsymbol{r}-\boldsymbol{r}_i)\,\Phi\, d^3\boldsymbol{r}_1\, d^3\boldsymbol{r}_2 \ldots d^3\boldsymbol{r}_A \tag{4.1}$$

$$N\rho_n(\boldsymbol{r}) = \int \Phi^* \sum_{j=1}^{N} \delta(\boldsymbol{r}-\boldsymbol{r}_j)\,\Phi\, d^3\boldsymbol{r}_1\, d^3\boldsymbol{r}_2 \ldots d^3\boldsymbol{r}_A \tag{4.2}$$

where the sums over i and j are over the proton and neutron coordinates respectively. Neglecting for the time being the magnetic part of the lepton–nucleon interaction, the static charge distribution which reproduces the potential in equation (2.26) is then

$$Z\rho(\boldsymbol{r}) = Z\int \rho_p(\boldsymbol{r}) g_p(\boldsymbol{r}-\boldsymbol{r}')\, d^3r' + N\int \rho_n(\boldsymbol{r}) g_n(\boldsymbol{r}-\boldsymbol{r}')\, d^3r \tag{4.3}$$

where g_p and g_n are the proton and neutron charge densities respectively.† The importance of including the neutron charge density has been pointed out by Bertozzi *et al* (1972) who also introduce an effective charge ρ_{eff} to simulate the contribution of the spin–orbit force which becomes most significant when a $j = l+\frac{1}{2}$ shell in the nucleus is fully occupied while the corresponding $j = l-\frac{1}{2}$ shell is unoccupied. Direct calculations of proton and neutron density distributions from nuclear theory have been reviewed by Bethe (1971).

4.1. The Hartree–Fock approximation

In the Hartree–Fock approximation the many-body wavefunction is assumed to be an anti-symmetrized product of single-particle wavefunctions. For sufficiently weak interparticle forces it can be shown that the energy is a minimum if each single-particle wavefunction describes the motion of the particle in the average field of all the other particles (see eg Brown 1971). This self-consistent field method works very well for atoms and the success of the shell model in describing many properties of nuclei suggests that it should be applicable to the latter. The nucleon–nucleon force, however, is not sufficiently weak. The strong tensor force and short-range part of the central force which cause the difficulty can be taken into account by doing a Brueckner–Hartree–Fock calculation which results in a 'rearrangement potential' as well as the self-consistent field. An alternative method due to Nemeth

† We assume that the charge densities have been modified to take account of relativistic effects of order v^2/c^2 due to the nucleon motion. (See eg appendix D of de Forest and Walecka 1966.)

and Ripka (1972) is to separate the potential energy into a volume term, which is adjusted to give the correct binding energy for infinite nuclear matter, and a residual surface term which has no adjustable parameters. This makes it possible to use the ordinary Hartree–Fock method. In these cases, however, we can no longer prove that the self-consistent solutions give the minimum energy, but it has been customary to assume that they do. Descriptions of Hartree–Fock calculations together with numerical results have been given recently by Vautherin and Vénéroni (1967, 1969), Negele (1970), Campi and Sprung (1972), Shao *et al* (1972) and Nemeth and Ripka (1972). Some examples are given in § 5. Both proton and neutron density

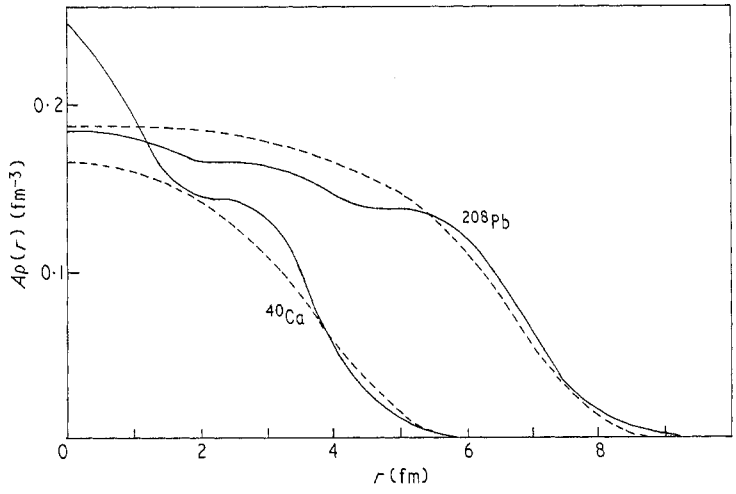

Figure 6. Nuclear matter (proton plus neutron) densities derived from Hartree–Fock (full lines) and Thomas–Fermi (broken line) calculations using a Brink and Boeker force (Lombard 1970).

distributions can be obtained from macroscopic calculations (ie those in which the coordinates of individual nucleons do not appear) in which the total energy is expressed as a function of the density. The latter is then varied to minimize the energy. Many of these calculations are reviewed in the following paper (Jackson 1974). In some of these the theory contains parameters which are adjusted to give the correct binding energy and equilibrium density. In later calculations the parameters were fixed by nuclear matter calculations (Bethe 1968). Lombard (1970) has carried out both Hartree–Fock and Thomas–Fermi calculations based on the same nucleon–nucleon force. The charge densities derived from the latter show the same over all features as the Hartree–Fock densities but give worse fits to electron scattering measurements. Examples of the difference between nuclear matter (proton plus neutron) densities obtained using the two different methods of calculation are shown in figure 6. (The Thomas–Fermi proton and neutron distributions are assumed to be identical in the calculation.) When the more realistic (density dependent) Skyrme force is used the oscillations in the Hartree–Fock densities are considerably reduced.

4.2. Semi-empirical single-particle model calculations

The earliest calculations of charge densities were carried out for light nuclei using harmonic oscillator wavefunctions (see eg Hofstadter 1957, Meyer-Berkhout

et al 1959). In these calculations the size parameter of the oscillator potential was adjusted to fit the scattering and in some cases different size parameters were used for the 1s and 1p shells. A much more elaborate approach applicable to medium and heavy nuclei was subsequently introduced by Elton and collaborators (Shaw *et al* 1965, Swift and Elton 1966, Elton and Swift 1967) and involved numerical solutions of the Schrödinger equation for protons moving in a Saxon–Woods potential:

$$V(r) = V_c - V_e f(r) + V_{se}\left(\frac{\hbar}{m_\pi c}\right)^2 \frac{1}{r}\frac{df}{dr} \boldsymbol{l}.\boldsymbol{\sigma} \tag{4.4}$$

where V_c is the coulomb potential and

$$f(r) = \left[\exp\left(\frac{r-R}{a}\right) + 1\right]^{-1}. \tag{4.5}$$

In the earliest calculations the strengths V_e and V_{se} of the central and spin–orbit parts of the potential were taken to be the same for all levels. The parameters of the potential were varied subject to the constraint that the single-particle energies agreed fairly well with proton separation energies until the resulting charge distribution gave the best fit to the electron scattering cross sections. It was subsequently found that if V_e and V_{se} were made energy-dependent to simulate the non-locality of a Hartree–Fock potential, it was possible to obtain better fits to the separation energies. This method does not allow much freedom in varying the shape of the charge distribution (Elton 1967a), which makes the successes of the method more impressive although some of the resulting parameters such as the diffuseness of the potential sometimes show unexpectedly large variations (eg Elton and Swift 1967). It was found, however, that the charge distributions would not fit very high energy scattering data and it became necessary to take account of correlations (or corrections to the Hartree–Fock approximation). Elton and Webb (1970) did this by introducing additional arbitrary parameters, but it is possible to introduce correlations without additional parameters as has been shown by Negele (1971). Recently Brueckner *et al* (1972) have investigated the question of obtaining a 'best' single-particle potential with rearrangement terms, and show that the resulting wavefunctions have maximal overlap with the true wavefunction. Examples of densities obtained from single-particle wavefunctions are given in § 5.

4.3. Centre of mass corrections

When single-particle model wavefunctions are used the motion which they describe includes a certain amount of motion of the centre of mass of the nucleus. This can also happen in Hartree–Fock calculations although it is possible to introduce a constraint to eliminate the centre of mass motion before the Hartree–Fock equations are solved. If the single-particle wavefunctions are harmonic oscillator wavefunctions, the correction is simply carried out, and where the Born approximation is valid the form factor is multiplied by an additional factor

$$\exp(q^2 b^2/4A)$$

where b is the harmonic oscillator length parameter ($\simeq$ 1–2 fm). The centre of mass and proton finite size corrections produce opposite effects and partly cancel each other for light nuclei. When the Born approximation is not valid both of these

corrections can be made by evaluating a single radial integral (Negele 1970, Campi and Sprung 1972). The ratio $b^2/4A$ does not fall rapidly for heavier nuclei but for these the cross section is negligibly small for values of the momentum transfer for which the centre-of-mass correction is important.

If the wavefunctions are not those of a harmonic oscillator then the problem of correcting for the centre-of-mass motion becomes difficult. It amounts to choosing the function $G(\boldsymbol{R})$ of the centre-of-mass coordinate $\boldsymbol{R}$ which relates the translation invariant wavefunctions $\Phi(\boldsymbol{r}')$ to the single-particle model wavefunctions $\Psi(\boldsymbol{r}'+\boldsymbol{R})$ (Lipkin 1958):

$$\Phi(\boldsymbol{r}') = \int \mathrm{d}^3R\, G(\boldsymbol{R})\, \Psi(\boldsymbol{r}'+\boldsymbol{R}). \tag{4.6}$$

Friar (1971) has calculated the correction for a number of different functions ranging from $G(\boldsymbol{R}) = 1$ (the Gartenhaus–Schartz transformation) to $G(\boldsymbol{R}) = \delta(\boldsymbol{R})$. The form factor for ^{4}He scattering was found to vary dramatically with the range of G. Similar results have been found by Ciofi degli Atti *et al* (1972) and many other authors. Recently Ernst *et al* (1973) have suggested that G should be chosen to minimize the expectation value of the intrinsic hamiltonian, which would give the maximum overlap between $\Phi(\boldsymbol{r}')$ and the exact ground state wavefunction. An alternative method is to include the effect of centre of mass motion in the operator whose expectation value gives the form factor, and make an expansion in one-, two- and many-body clusters (eg Grypeos 1969). Failure to allow correctly for the effect of centre of mass motion has invalidated many calculations.

4.4. Correlations

If we define a two-particle proton density by the formula

$$Z(Z-1)\,\rho_{\mathrm{p}}(\boldsymbol{r},\boldsymbol{r}') = \int \Phi^* \sum_{i\neq j}^{Z} \delta(\boldsymbol{r}-\boldsymbol{r}_i)\,\delta(\boldsymbol{r}'-\boldsymbol{r}_j)\,\Phi\,\mathrm{d}^3r_1\,\mathrm{d}^3r_2 \ldots \mathrm{d}^3r_A \tag{4.7}$$

then we say that the proton motion is correlated if we obtain a non-zero value for the correlation function given by

$$C(\boldsymbol{r},\boldsymbol{r}') = \rho_{\mathrm{p}}(\boldsymbol{r},\boldsymbol{r}') - \rho_{\mathrm{p}}(\boldsymbol{r})\,\rho_{\mathrm{p}}(\boldsymbol{r}') \tag{4.8}$$

and when such correlations are taken into account the predicted cross sections may be considerably altered. Various factors contribute to the correlation function: the anti-symmetry of the wavefunctions results in the so-called Pauli correlations which have a long range; the tail of the nuclear force also produces long-range correlations, while the short-range part produces short-range correlations. The result is that the wavefunction is no longer a single Slater determinant of single-particle wavefunctions, but rather an infinite linear combination of such determinants. If the single-particle wavefunctions come from a self-consistent Hartree–Fock potential then there will be no component in the wavefunction corresponding to one-particle one-hole (1p–1h) excitations. There will, however, be components corresponding to 2p–2h, 3p–3h, 4p–4h, etc excitations and these will affect the one-body density $\rho(\boldsymbol{r})$.

One way of trying to take account of the short-range correlations is to introduce a Jastrow correlation function, i.e. to multiply the determinant by a factor

$$\prod_{i<j} f(|\boldsymbol{r}_i-\boldsymbol{r}_j|) \tag{4.9}$$

where the function f has the properties

$$f(0) = 0 \tag{4.10}$$

$$f(\infty) = 1. \tag{4.11}$$

This method has been used by several authors to improve the fit to electron scattering cross sections obtained from single-particle wavefunctions (Czyż and Leśniak 1967, Khanna 1968, 1971, Ciofi degli Atti 1969, 1971, Gerace and Sparrow 1969, Ciofi degli Atti and Kabachnik 1970). The improvement obtained has sometimes been quoted as evidence for the existence of two-body correlations in nuclei. It has been pointed out, however, that one of the most important effects of the Jastrow correlation function is to introduce 1p–1h excitations into the wavefunction, ie to change the single-particle basis states (Ripka and Gillespie 1970, Gaudin *et al* 1971, Fink *et al* 1971). In addition the functional form and range of $f(r)$ are not known so that it is difficult to draw any quantitative conclusions from the improved fits to the scattering.† One useful feature of the Jastrow factor is the fact that it is translationally invariant, so that it does not change the centre of mass component of a wavefunction (Ciofi degli Atti *et al* 1972). In view of the difficulties of correcting for this motion (described in § 4.3) this means that the Jastrow method could be useful if a proper theoretical form were found for the function $f(r)$.

5. Experimental results and comparisons between theoretical and experimentally derived charge distributions

The preceding analysis has indicated that in most cases we obtain information about the charge distribution in an indirect way, namely by assuming a particular form of the distribution and then calculating the scattering cross section or atomic spectrum. In many cases the shape is taken to be a simple function $\rho_j(\boldsymbol{r}, x_1, x_2, \ldots)$ of the position vector $\boldsymbol{r}$ and a number of size and shape parameters x_i. The calculation is repeated with different values of the parameters which are systematically adjusted to give a good fit to the experiment. The result of this, to take a sceptical view, is that we can say we have found one member of the infinite subset of charge distributions which are consistent with the experimental data. The possibility of saying something more definite about the charge distribution depends on our intuition and on knowledge from other sources. An increasing number of parameters has been used in the function ρ_j as the accuracy and energy range of the experiments have increased. The earliest electron scattering experiments were at low energy and the results could be reproduced by any distribution with the right mean square radius (Bodmer 1953) and there was therefore nothing to distinguish between extremes such as an exponential shape and a uniform charge distribution or even a spherical shell. Our intuition enables us to eliminate discontinuous functions, and the near constancy of the nuclear binding energy per nucleon suggests that one of the gross features of the distribution should be an approximately constant density. The suggestion was confirmed when higher momentum transfer experiments for heavy nuclei showed a diffraction pattern which ruled out exponential and gaussian shapes, and indicated some sort of edge to the nucleus

† There has been some disagreement in the literature about the extent to which it is meaningful to compare Jastrow and Brueckner correlations (see eg Ciofi degli Atti 1971). In view of the arbitrariness of the former, however, and the fact that the Jastrow method changes the single-particle basis, this does not seem to be an important question.

(Ravenhall and Yennie 1954). A number of different two-parameter radial distributions were used successfully by various authors (Yennie *et al* 1954, Brown and Elton 1955) and these gave a density which was more or less constant in the interior and had a diffuse edge. Gradually the fermi distribution $\rho = \rho_0\{\exp[(r-c)/a]+1\}^{-1}$ became more popular than other two-parameter shapes and remained so until very recently.

The early analyses in terms of two-parameter distributions did give the gross features of the charge distribution in a model independent way. Subsequently there developed a tendency to attach much more significance to the resulting shapes than was justified. This is illustrated by recent analyses of electron scattering by ^{208}Pb. Heisenberg *et al* (1969a) started with several different functional forms for the density and fitted the low-q cross sections. After varying the parameters to fit the data they found that the resulting radial shapes were indistinguishable and concluded that they really had established certain features such as a central depression and a rapid fall-off in the tail (faster than the exponential fall-off of a fermi distribution). A different analysis by Friedrich and Lenz (1972) showed that both a central hump and a depression were consistent with 124 and 167 MeV data. Although the data used covered a smaller range of q values, the implication was that the choice of initial functions by Heisenberg *et al* was too restricted. This was confirmed by a recent exhaustive analysis of ^{208}Pb using electron scattering data at five different energies and muonic data. The results showed that ^{208}Pb may have a small central depression but that this conclusion is altered by very slight changes in the normalization of the scattering cross sections (Friar and Negele 1973). A qualitative fit to the data is obtained from the Hartree–Fock calculations of Faessler *et al* (1972), who find the usual hump in the centre. Friedrich and Lenz used a novel method of choosing a very large variety of distributions and obtained very good fits with distributions which looked strikingly different from those which had been put forward previously. They were also able to find certain integral functions of the charge distribution which differed very little amongst the hundreds of different densities which they had calculated, thus suggesting that these integral functions were really what the experiments were determining. Friar and Negele examined the exact form of the integral functions using perturbation theory and obtained the density in terms of an orthogonal set of functions. Their method also gave the statistical error in the density. Both of these methods are described in appendix 1.

In analyses of muonic x ray experiments it is more obvious that integral properties of the charge are being measured and for very light nuclei this quantity is the mean square radius $\langle r^2\rangle$ (for the 2P–1S transition). For heavy nuclei a very different moment is determined and Hill and Ford (1954) found that for lead it was approximately the $\langle r^{0.5}\rangle$ moment. More elaborate calculations by Ford and Wills (1969) appeared to show that a moment $\langle r^k\rangle$ was very accurately determined for many transitions. Here k was different for each transition and varied with Z. It subsequently turned out that the integral property which was really determined would be much more accurately represented by the generalized moment $\langle r^k e^{-\alpha r}\rangle$ where α is also a function of Z (Barrett 1970, Rinker 1971a, Ford and Rinker 1972). Although muonic x ray energies do not give any nuclear size information other than the determination of the generalized moments, it has been customary to analyse the experiments using fermi-type charge distributions, mainly due to the popularity of these distributions in electron scattering analyses. The errors quoted on the half-density radius, the skin thickness and the root mean square radius are not

meaningful, ie different values would be obtained if a different functional form for the density were used. In ^{208}Pb the quoted error of less than 0·1% in the RMS radius is probably at least a factor of 10 too small (Rinker 1971b). Only the generalized moment $\langle r^{2\cdot46}\,e^{-0\cdot17r}\rangle$ is determined to this accuracy.

Since the charge distributions which result from fitting electron scattering and muonic x ray experiments depend strongly on the initial assumptions about the functional form of the distributions, one may ask whether it is possible to say anything about the density distribution apart from giving the generalized moments and other integral quantities. We believe that one may have more confidence in doing so when theoretical densities (based on some dynamical model of nuclear structure) give agreement with the experiments. At present theoretical calculations usually do have some adjustable parameters and do not fit the experiments perfectly. Nevertheless a rather small adjustment to the density (perhaps not even visible on a graph) is sometimes enough to bring about agreement. Thus it seems reasonable to suggest that the present theoretical distributions may be beginning to approach the 'true' distributions.

In spite of the limitations of phenomenological densities we reproduce them below for some nuclei (or give the parameters) and also give root mean square radii. The reason is that we often want to know the parameters or the RMS radius only approximately and for some purposes they may be determined sufficiently accurately despite the model dependence of phenomenological analyses. The radii and parameters given below all refer to *charge* densities and not proton densities.

5.1. Light nuclei

In this and the following sections we give typical results for selected nuclei rather than a compilation of all known experiments and analyses. Such compilations have been given by Hofstadter and Collard (1967), Elton (1967b) and Überall (1971). For these nuclei atomic levels are not very sensitive to the nuclear size and we discuss only electron scattering experiments.

^{4}He

The electron scattering for a range of q from 0·7 to 4·5 fm^{-1} has been measured by Frosch *et al* (1967) and the cross section showed a diffraction minimum which ruled out the previously assumed gaussian shape. The results were fitted with a parabolic fermi distribution with the parameters shown in table 3 as well as with the form factor

$$F(q^2) = [1-(a^2q^2)^6]\exp(-bq^2) \tag{5.1}$$

with $a = 0{\cdot}316$ fm and $b = 0{\cdot}681$ fm.†

A single-particle model calculation with adjustable parameters has been carried out by Frosch (1971) and a Hartree–Fock calculation (in which the parameters had been obtained from calculations for other nuclei) by Campi *et al* (1972). The cross sections and charge distributions are shown in figure 7.

^{12}C

The results for this nucleus are particularly important because in many experiments the ratio of the cross section to the ^{12}C cross section is measured. Bentz

† Throughout this section the unit of length is 1 fm = 10^{-13} cm.

Table 3. Parameters of phenomenological charge distributions† and root mean square radii‡

Nucleus	Particle used in experiment	Energy of electron in scattering experiments (MeV)	n	c	a	w	$\langle r^2\rangle^{1/2}$	Ref.
^{4}He	e	100–800	1	1·008	0·327	0·445	1·71	a
	e	30–60					2·40 (3)	b
^{12}C	e	20–80					2·453 (8)	c
	μ						2·454 (40)	u
^{16}O	e	375–750	1	2·608	0·513	−0·051	2·73	d
^{40}Ca	e	20–60	1	3·650	0·517	0	3·42	e
	e	250	1	3·6758	0·5851	−0·117	3·49	f
	e, μ	500	1	3·697	0·587	−0·083	3·53	f
	e	750	1	3·6685	0·5839	−0·1017	3·48	g
^{48}Ca	e	20–60	1	3·650	0·498	0	3·38	e
	e	250	1	3·7444	0·5255	−0·03	3·48	f
	e, μ	500	1	3·797	0·534	−0·048	3·52	f
	e	750	1	3·7369	0·5245	−0·03	3·47	g
^{90}Zr	e	300	2	4·434	2·528	0·350	4·27	h
	e	209, 302	2	4·45	2·54	0·28	4·27	i
^{120}Sn	e	150	1	5·315	0·575	0	4·64	j
	μ	—	1	5·495	0·507	0	4·66	k
^{138}Ba	e, μ	120, 500	2	5·3376	2·6776	0·3749	4·84	l
	μ	—	1	5·771	0·496	0	4·84	m
	e	40–60	1	5·83	0·407	0	4·77	n
^{142}Nd	e	500	1	5·6135	0·5868	0·0965	4·92	o
	e, μ	130, 200 300, 500	2	5·3120	2·7311	0·4378	4·89	l
^{208}Pb	μ	—	1	6·712	0·481	0	5·50	o
	μ	—	1	6·6592	0·5142	0	5·50	p
	μ	—	1	6·7202	0·5045	−0·061	5·50	p
	e	175	1	6·47	0·523	0	5·38	q
	e	175	1	6·38	0·537	0·130	5·39	q
	e	175, 250	1	6·40	0·542	0·140	5·42	q
	e	53	1	6·66	0·503	0	5·48	r
	e	124, 167	1	6·597	0·550	0	5·50	s
	e	124, 167	1	6·628	0·544	−0·062	5·4	s
	e, μ	248, 502	2	6·3032	2·8882	0·3379	5·50	t
	e	248, 502	2§	6·4745	2·975	0·361	5·50	t
	e	124, 167	2	6·529	2·813	0	5·44	s
	e	124, 167	2	6·437	2·849	0·163	5·48	s
	e	124, 167	δ¶				5·49 (9)	s

a, Frosch *et al* 1967
b, Bentz 1969
c, Jansen *et al* 1972
d, Sick and McCarthy 1970
e, Eisenstein *et al* 1969
f, Frosch *et al* 1968
g, Bellicard *et al* 1967
h, Fajardo *et al* 1971
i, Phan Xuan Ho *et al* 1972
j, Barreau and Bellicard 1967
k, Martin *et al* 1973
l, Heisenberg *et al* 1971a
m, Madsen *et al* 1971
n, Heisenberg *et al* 1971b
o, Anderson *et al* 1969
p, Kessler 1971
q, Bellicard and van Oostrum 1967
r, van Niftrik 1969
s, Friedrich and Lenz 1972
t, Heisenberg *et al* 1969a

† The phenomenological densities are of the form

$$\rho(r) = \frac{\rho_0(1+w(r/c)^2)}{\{\exp[(r^n-c^n)/a^n]+1\}}.$$

‡ Note that model dependence in phenomenological densities causes uncertainties of at least 1% in RMS radii.

§ The parabolic term wr^2/c^2 was divided by $\{\exp[(r^2-c^2)/a^2]+1\}$.

¶ The distribution used was a sum of spherical shells.

(1969) obtained a root mean square radius of $2{\cdot}40 \pm 0{\cdot}03$ fm from measurements with q ranging from 0·1 to 0·5 fm^{-1}. Recently Jansen *et al* (1972) obtained the value $2{\cdot}453 \pm 0{\cdot}008$ fm from measurements with q ranging from 0·15 to 0·7 fm^{-1}. If this new measurement is accepted, then this alters the cross section for other nuclei in the cases where the measurement was made as a ratio to the ^{12}C cross section. This

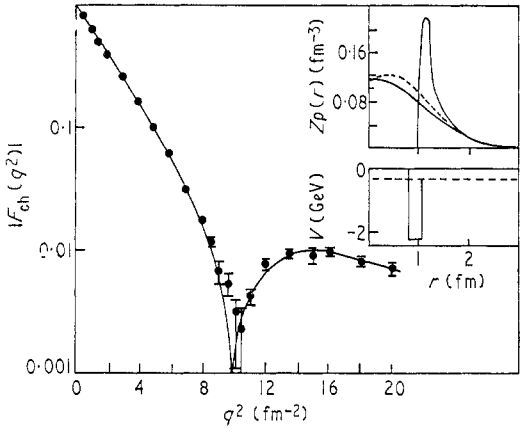

Figure 7. The ^{4}He charge form factor and densities. The experimental points and the continuous curve from the phenomenological density shown are from Frosch *et al* (1967). The broken curve is obtained from the strongly peaked square wavefunction calculated using the potential shown by folding in the finite size and centre of mass corrections (Frosch 1971).† (Note that the latter cannot be obtained in a unique way as shown in § 4.3.)

means for example that the RMS radii obtained by van Niftrik (1969) for Pb and Bi are increased by 0·03 fm (Jansen *et al* 1972). The new RMS radius is in good agreement with that obtained from a recent CERN muonic x ray measurement (Backenstoss *et al* 1973).

^{16}O

Measurements have been made by Sick and McCarthy (1970) for $q = 1$ to $q = 4$ fm^{-1}, and single-particle model (Saxon–Woods) densities have been found to give a moderately good fit by Donnelly and Walker (1969). A similar fit has been obtained using an α particle cluster model for ^{16}O by McDonald and Überall (1970). These calculations reproduce the second diffraction minimum while harmonic oscillator wavefunctions do not. The fit can be dramatically improved by introducing Jastrow correlations into the wavefunction (Ciofi degli Atti and Kabachnik 1970). However, as pointed out in § 4.4, the additional parameters involved introduce an arbitrariness into the resulting density.

5.2. Medium and heavy closed shell nuclei

We shall confine most of our attention to this small class of nuclei because of the large number of experimental and theoretical studies that have been made of them and because of the greater uncertainties involved in obtaining information about the charge in other nuclei due to the model dependence of phenomenological analyses and the difficulty of the theoretical calculations. Some additional results are given in the sections on isotope shifts (5.3) and isotone shifts (5.4).

† The author is indebted to I. Sick for providing the folded curve.

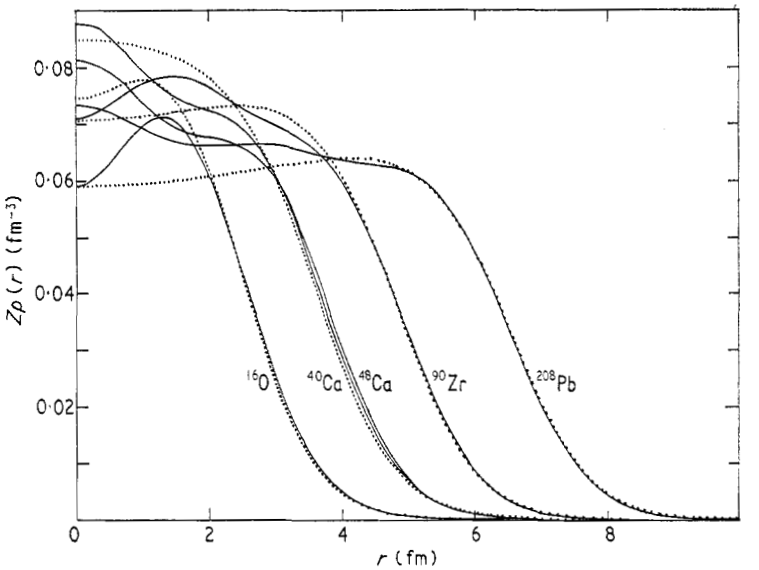

Figure 8. Phenomenological and Hartree–Fock densities for closed shell nuclei. The theoretical densities are from the Hartree–Fock calculations of Campi and Sprung (1972), while the phenomenological densities (shown as broken curves) are from the following sources: ^{16}O Ehrenberg *et al* (1959), ^{40}Ca Frosch *et al* (1968), ^{90}Zr Fajardo *et al* (1971), ^{208}Pb Heisenberg *et al* (1969a).

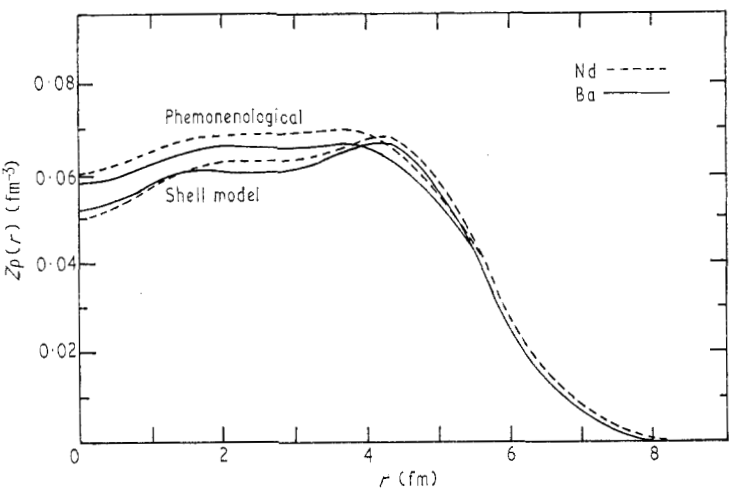

Figure 9. Phenomenological and single-particle shell model densities for ^{138}Ba and ^{142}Nd (Heisenberg *et al* 1971a).

In figure 8 we show theoretical and phenomenological densities for ^{16}O, ^{40}Ca, ^{48}Ca, ^{90}Zr and ^{208}Pb. The theoretical curves are from Hartree–Fock calculations of Campi and Sprung (1972) and are almost identical with those obtained by Negele (1970).

Figure 9 shows phenomenological and single-particle shell model densities for ^{138}Ba and ^{142}Nd obtained by Heisenberg *et al* (1971a). There is good agreement in the region of steepest slopes which is the region where the accuracy of phenomenological densities is expected to be greatest.

^{40}Ca and ^{48}Ca

The phenomenological analysis of electron scattering was carried out with a two- and then a three-parameter function for data up to 250 MeV (van Oostrum *et al* 1966). When the experiments were extended to 750 MeV ($q_{max} = 3{\cdot}2$ fm^{-1}) it was necessary to introduce undulations into the charge distribution which was done by adding a modification $\Delta\rho(r)$ which had no Fourier component below $q = 2{\cdot}5$ fm^{-1} and did not affect the cross section in this region (Frosch *et al* 1968). The form of the charge distribution used had a total of six adjustable parameters. Semi-empirical densities were obtained by Elton and Webb (1970) using a non-local potential but they found that whatever potential parameters they used the density which resulted had too much undulation to fit the high-q data if only the

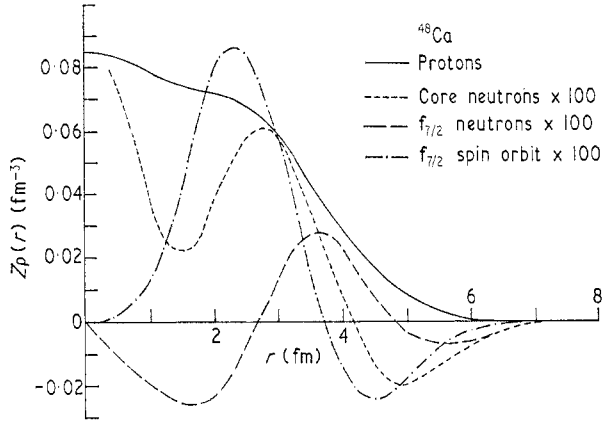

Figure 10. The proton density, the charge density due to the neutron form factor and the effective charge density resulting from the spin–orbit force between electrons and $f_{7/2}$ neutrons (Bertozzi *et al* 1972).

lowest energy states were filled. They were able to obtain a good fit by including two particle–two hole correlations corresponding to promoting a total of 1·5 protons into the 2p–1f shell. The amount of correlation added was adjustable to fit the cross sections. One result which came from both electron scattering and muonic x ray experiments (Ehrlich *et al* 1967) is the fact that the RMS radius of the phenomenological charge density is smaller for ^{48}Ca than for ^{40}Ca, whereas Hartree–Fock calculations indicate that it should be larger. This was somewhat surprising even taking into account the uncertainties in the phenomenological analyses. The puzzle has been solved by Bertozzi *et al* (1972) who calculated the contribution from the neutron charge form factor and the spin–orbit interaction between the electron and the $1f_{7/2}$ neutrons in ^{48}Ca. These effects produced a negative shift of 0·021 fm compared with the phenomenological decrease of 0·009 fm, ie the results indicated that the radius of the proton distribution *increased* by 0·012 fm. This is to be compared with the increase of 0·04 fm obtained by Negele (1970) and 0·02 fm by Campi and Sprung (1972) from Hartree–Fock calculations. The charge density due to the neutrons and the effective charge which simulates the spin–orbit interaction between the electron and the $1f_{7/2}$ neutrons is shown in figure 10.

^{208}Pb

Electron scattering measurements for $q = 0{\cdot}15$ to $0{\cdot}53$ have been reported by van Niftrik (1969), for $q = 0{\cdot}6$ to $1{\cdot}6$ by Friedrich and Lenz (1972) and for $q = 0{\cdot}7$

to 2·7 fm^{-1} by Heisenberg *et al* (1969a). Very accurate muonic x ray measurements have been carried out by Anderson *et al* (1969) and by Jenkins *et al* (1971). Some of the phenomenological densities as well as the semi-phenomenological density of Elton *et al* (1969) gave the rather small value of about 5·42 fm for the RMS radius, whereas analysis of muonic x ray spectra gave 5·50 fm (or 5·51 fm if nuclear polarization effects are included (Kessler 1971)). This discrepancy is almost certainly due mainly to model dependence in the analysis of muonic x ray and electron scattering experiments and Heisenberg *et al* were able to fit both kinds of experiment simultaneously (obtaining an RMS radius of 5·50 fm). These authors used a

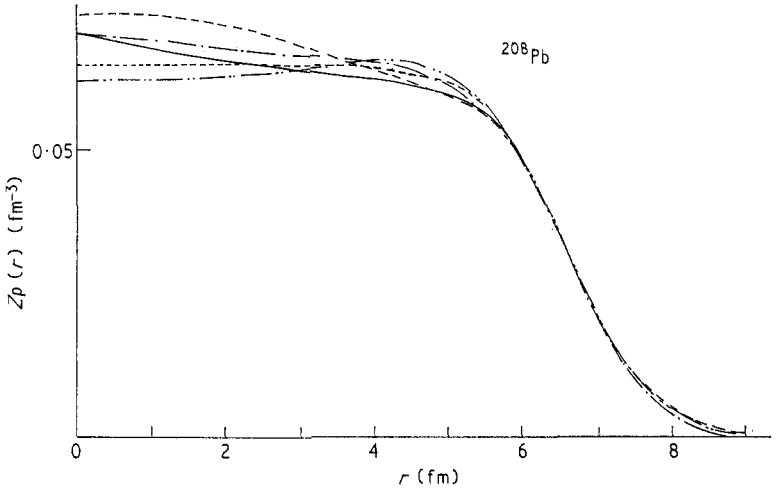

Figure 11. Phenomenological densities (Friedrich and Lenz 1972) and a Hartree–Fock density (Campi and Sprung 1972) for ^{208}Pb (full line). The curve with the lowest central density is that of Heisenberg *et al* (1969a).

three-parameter shape to fit the low-q data (as for ^{40}Ca and ^{48}Ca) and added a three-parameter oscillation which affected only the high-q cross sections. Their resulting density, together with a number of other charge distributions found by Friedrich and Lenz (1972), is shown in figure 11. Friedrich and Lenz found a RMS radius of $5{\cdot}49 \pm 0{\cdot}09$ fm, a mean radius $\langle r \rangle$ of $5{\cdot}23 \pm 0{\cdot}05$ fm and a squared mean root radius $\langle r^{1/2} \rangle^2$ of $4{\cdot}94 \pm 0{\cdot}06$ fm.

The muonic x ray experiments have been analysed in a model independent way by Ford and Rinker (1972) who calculated generalized moments $\langle r^k e^{-\alpha r} \rangle$. They plotted the radius of the equivalent uniform distribution against k and the result is shown in figure 12. The experimentally determined values of R_k place a constraint on possible charge distributions. A complete determination would require precise values of R_k for an infinite set of k. It is interesting to compare different charge distributions by plotting their R_k against k curves and comparing them with the muonic x ray results. Inconsistencies in the latter, whether due to experimental error or neglected theoretical corrections, are revealed by departures from a smooth curve. This is the case for the point at $k = 4{\cdot}6$ which comes from the $3D_{3/2}$–$3D_{5/2}$ energy difference. A model independent analysis of electron scattering and muonic x ray measurements has recently been carried out by Friar and Negele (1973).

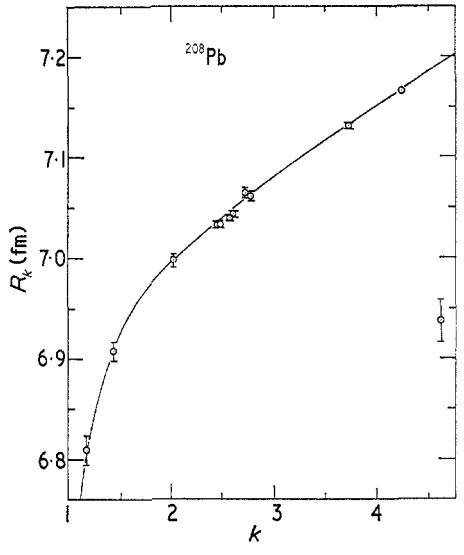

Figure 12. Equivalent radii R_k for generalized moments $\langle r^k e^{-\alpha r}\rangle$ with $\alpha = 0{\cdot}17$ fm^{-1}. The circles are obtained from the measured x ray energies and the continuous curve corresponds to a phenomenological density which fits these energies and is also very close to that obtained from the analysis of electron scattering cross sections. The figure is taken from Ford and Rinker (1972).

5.3. Isotope shifts

In optical and electronic x ray transitions the field shift is very nearly proportional to $\delta\langle r^2\rangle$† and it is convenient to express this in terms of a 'standard shift' based on an equivalent uniform charge density of radius $R_{eq} = r_0 A^{1/3}$ fm. This standard unit of isotope shift does not have a fundamental significance but does represent approximately the overall variation of R_{eq} *for stable nuclei.* Because a change in neutron number is either a move towards or away from the region of stability there is no reason to expect isotope shifts to be the same as the standard shift and in fact they are usually smaller. Some of the exceptions are due to changes in the deformation for non-spherical nuclei and it was in fact these unusually large shifts which led to the discovery of intrinsic deformations in spin 0 nuclei (Brix and Kopfermann 1949). The use of the standard shift also occurs in the analysis of muonic x ray data where calculations are quoted for the change in x ray energy corresponding to a fermi distribution whose RMS radius is proportional to $A^{1/3}$ and whose skin thickness is constant.

A more complicated dependence on A, with terms proportional to $A^{1/3}$, $A^{-1/3}$ and A^{-1}, has been presented by Elton (1961). This was based on several assumptions: the proton and neutron densities have the same size and shape; the shape is that of a fermi distribution; the central density $A\rho(0)$ is the same for all nuclei. This sort of analysis was of value in showing departures from the simple $A^{1/3}$ dependence. Now that phenomenological shapes have more parameters (and the fermi distribution is in any case out of favour), and because of model dependence in phenomenological analyses, such formulae are no longer appropriate.

† The standard shift calculated on the basis of a $\delta\langle r^2\rangle$ dependence can be corrected by dividing by the quantity $[1+1{\cdot}2\times10^{-5}Z^2]$. This correction takes into account the effect of $\delta\langle r^4\rangle$ and $\delta\langle r^6\rangle$ terms and is based on the results of Seltzer (1969).

There are now available a large number of experimental results on very many isotopes. Only a few of these are discussed below and they have been selected because of particularly intensive experimental studies, involving different kinds of experiments, or because of their theoretical interest. Results for many other isotopes have been given by Stacey (1966), Ehrlich (1968), Macagno *et al* (1970) and Boehm (1972).

When phenomenological charge densities are used in the analysis of differences between isotopes it is reasonable to expect the model dependence to be less important than it is in the analysis of a single density, especially in the calculation of overall quantities such as the mean square radius. The fact that isotope shifts are the small differences between large quantities means that small theoretical corrections may have a dramatic effect on the conclusions about changes in the charge distributions. Wall (1971) has shown that in the case of low-q electron scattering experiments on Ti isotopes, the effect on the cross sections of changes between different isotopes in the dispersion correction is of the same order of magnitude as the effect due to the changes in the charge distribution. Changes in the nuclear polarization correction to muonic atom levels can be equally dramatic for all except the S states as can be seen from the results of Macagno *et al* (1970).

5.3.1. Ca isotopes. Measurements of electron scattering at 250 and 500 MeV have been carried out by Frosch *et al* (1968) for Ca isotopes of mass number 40, 42, 44 and 48. Muonic x ray measurements have been reported by Ehrlich (1968) for

Table 4. Ca isotope shifts

Isotope pair	$(\delta E)_{\text{field}}/(\delta E)_{\text{std}}$[a] from muonic x rays	$\delta\langle r^2\rangle$ (fm^2) from electron scattering	$\delta r_{0\cdot5}$ (fm) from electron scattering[b]
40–42	0·48 (4)[c]	0·21[e]	0·03[e]
40–44	0·33 (2)[c] 0·36 (4)[d]	0·20[e]	0·08[e]
40–48	−0·01 (4)[c]	−0·07[e] −0·26[f]	0·16[e] 0·07[f]

a, standard shift based on uniform charge distribution of radius $1{\cdot}2A^{1/3}$ fm.
b, the quantity $r_{0\cdot5}$ is the radius at half maximum density.
c, Ehrlich 1968
d, Macagno *et al* 1970
e, Frosch *et al* 1968
f, Eisenstein *et al* 1969

mass numbers 40, 42, 44 and 48. The muonic x ray shift for ^{40}Ca–^{48}Ca has also been measured by Macagno *et al* (1970). These results are in reasonable agreement and are summarized in table 4. Both types of experiment show a negative shift between ^{40}Ca and ^{48}Ca. Phenomenological densities consistent with these results show an increase in half-density radius ($r_{0\cdot5}$) and a decrease in skin thickness between ^{40}Ca and ^{48}Ca.†

5.3.2. Zr isotopes. Electron scattering measurements at 300 MeV have been made by Fajardo *et al* (1971) for Zr isotopes of mass number 90, 91, 92, 94 and 96.

† In this and the following tables $\delta\langle r^2\rangle$ is taken to be *positive* if the heavier isotope has the larger mean square radius.

Results of muonic x ray measurements have been given by Ehrlich (1968) for ^{90}Zr and ^{92}Zr and optical measurements for mass numbers 90, 92, 94 and 96 have been made by Heilig *et al* (1963) (see table 5). There is some disagreement between the optical and electron scattering mean square radii, but this is not significant since the electron experiments are at fairly high momentum transfer.

Table 5. Zr isotope shifts and changes in mean square radius

Isotope pair	$(\delta E)_{\text{field}}/(\delta E)_{\text{std}}$[a]		$\delta\langle r^2\rangle$ (fm^2) from electron scattering[b e]
	Muonic[c]	Optical[d]	
90–91			0·30
90–92	1·14 (6)	1·10 (12)	0·22
92–94		0·78 (12)	0·28
94–96		0·61 (13)	0·56

a, standard shift based on uniform charge distribution of radius $1{\cdot}2A^{1/3}$ fm.
b, the standard shift for the addition of two neutrons is approximately 0·25 fm^2.
c, Ehrlich 1968
d, Heilig *et al* 1963
e, Fajardo *et al* 1971

5.3.3. Sn isotopes. The ten stable isotopes of Sn have been the subject of a large number of studies. Optical measurements on all of them have been made recently (Silver and Stacey 1973) for mass numbers 116, 117, 118, 119, 120, 122 and 124, and Goble and Silver (1973) for mass numbers 112, 114 and 115). Electron scattering cross sections at 330 MeV on all except ^{115}Sn have been made by Ficenec *et al* (1972); at 225 MeV for mass numbers 116, 118 and 124 by Litvinenko *et al* (1972); at 150 MeV for mass numbers 116, 120 and 124 by Barreau and Bellicard (1967). Muonic x ray measurements for the isotopes of mass number 116 to 124 were made by Macagno *et al* (1970) and measurements for the even isotopes in this group were reported by Ehrlich (1968). Electronic x ray measurements for ^{116}Sn and ^{124}Sn were made by Chesler and Boehm (1968). Results are summarized in table 6.

5.3.4. Nd isotopes. Measurements of x rays in electronic atoms have been made by Bhattacherjee *et al* (1969) and in muonic atoms by Macagno *et al* (1970) for mass numbers 142, 143, 144, 145, 146, 148 and 150. Heisenberg *et al* (1971b) have carried out electron scattering experiments at 130, 200, 300 and 500 MeV for mass numbers 142, 144, 146, 148 and 150. Some of the results are given in table 7. The slightly higher values of the ratio for muonic shifts are to be expected since for $Z = 60$ there is a considerable fall-off in the 1S wavefunction between the centre and the edge of the nucleus.

5.3.5. Pb isotopes. Electron scattering measurements for q in the range 0·2 to 0·9 fm^{-1} have been made on isotopes of mass number 206, 207 and 208 by de Jager *et al* (1972). Optical measurements on all the even isotopes in the range 204 to 210 were made by Steudel (1952). Isotopes 204, 206, 207 and 208 have been studied by Boehm and Lee (1972) who measured electronic x ray energies and by Anderson *et al* who measured muonic x ray energies (Kessler 1971). A very detailed analysis of the muonic results has been carried out by Ford and Rinker (1972). Results are given in table 8.

Table 6. Sn isotope shifts

Isotope pair	$(\delta E)_{field}/(\delta E)_{std}$[a]		$\delta\langle r^2\rangle$ (fm^2)	
	Muonic	Electronic	Optical†	Electron scattering
114–115		0·38 (3)[f]	0·045[f]	
116–117	0·46 (2)[b]	0·42 (3)[e]	0·049[e]	0·055[g]
	0·45 (2)[c]			
118–119	0·35 (4)[b]	0·38 (3)[e]	0·045[e]	
112–114		0·54 (4)[f]	0·129[f]	0·147[g]
114–116		0·56 (4)[e, f]	0·133[e, f]	0·157[g]
116–118	0·60 (1)[b]	0·53 (4)[e]	0·124[e]	0·139[g]
	0·63 (2)[c]			
118–120	0·52 (1)[b]	0·48 (4)[e]	0·112[e]	0·111[g]
120–122	0·45 (2)[b]	0·43 (3)[e]	0·101[e]	0·112[g]
122–124	0·45 (1)[b]	0·39 (3)[e]	0·091[e]	0·112[g]
116–120		0·50 (4)[e]	0·236[e]	
120–124		0·41 (6)[e]	0·192[e]	
116–124	0·503 (5)[b]	0·458[e]	0·428[e]	0·206[g]
		0·458 (17)[d]		

† Note that the shifts are normalized by the electronic K x ray measurement of the 116–124 shift.[d]

a, standard shift based on uniform charge density of radius $1{\cdot}2A^{1/3}$ fm.
b, Macagno *et al* (1970)
c, Ehrlich 1968.
d, Bhattacherjee *et al* (1969)
e, Silver and Stacey 1973
f, Goble and Silver 1973
g, values mainly from electronic x ray results were used as a constraint in fits to electron scattering by Ficenec *et al* 1972.
h, Litvinenko *et al* 1972

Table 7. Nd isotope shifts

Isotope pair	$(\delta E)_{field}/(\delta E)_{std}$[a]			$\delta\langle r^2\rangle$ (fm^2)	
	Muonic[b]	Optical[c]	Electronic[d] x rays	Optical[c]	Electron scattering[e]
142–143			0·84 (7)	0·092 (10)	
144–145			0·26 (15)	0·028 (20)	
142–144	1·22 (1)	1·04 (5)	1·40 (6)	0·307 (16)	0·346
144–146	1·18 (1)	1·00 (4)	1·11 (13)	0·243 (34)	0·119
146–148	1·34 (1)	1·09 (5)	1·31 (13)	0·286 (35)	0·219
148–150	1·79 (2)	1·59 (6)	1·92 (8)	0·420 (20)	

a, standard shift based on a uniform distribution of radius $1{\cdot}20A^{1/3}$ fm.
b, shifts in the 1S level obtained by Macagno *et al* (1970).
c, shifts for the 5675 Å line measured by Gerstenkorn and Helbert (1968) with a specific mass shift of -15 mK (0·015 cm^{-1}) which was also used to calculate $\delta\langle r^2\rangle$ (Stacey 1971).
d, from Bhattacherjee *et al* (1969) with the standard shift of 0·050 eV based on results of Seltzer (1969).
e, from experiments and analysis of Heisenberg *et al* (1971a), who also obtain good fits when the densities are constrained to fit the $\langle r^2\rangle$ values from optical or electronic x ray experiments.

Table 8. Pb isotope shifts

Isotope pairs	$(\delta E)_{field}/(\delta E)_{std}$ Optical[a]	Electronic[b] x ray	$\delta\langle r^2\rangle$ (fm^2) Electronic x ray[c]	$\delta R/\delta R_{std}$ from muonic x rays[d] $3P_{3/2}$–2S	$2P_{3/2}$–1S	$3D_{5/2}$–$2P_{3/2}$
206–207		0·29 (11)	0·028 (12)	0·58 (26)	0·483 (21)	0·594 (87)
204–206	0·53 (6)	0·54 (11)	0·106 (23)	0·76 (13)	0·64 (7)	0·704 (35)
206–208	0·60 (7)	0·55 (7)	0·109 (14) 0·11 (4)	0·69 (14)	0·611 (7)	0·726 (35)
208–210	1·05 (12)					

a, Steudel 1952

b, the standard shift based on results of Seltzer (1969) is 0·341 eV for 206 to 208. The experimental results are from Boehm (1972).

c, the values of $\delta\langle r^2\rangle$ are larger than those quoted by Boehm because an estimate has been made of the correction due to $\langle r^4\rangle$ and $\langle r^6\rangle$ moments (based on a uniform charge distribution).

d, the values of δR give the changes in the radius of the equivalent uniform distribution, ie that which has the same value of the generalized moment $\langle e^{-0\cdot17r}\, r^k\rangle$. They are taken from the calculation of Ford and Rinker (1972) based on measurements quoted by Kessler (1971).

5.3.6. Discussion. The values of $\delta\langle r^2\rangle$ obtained from different types of experiments are, in general, consistent. Not much additional information can be obtained from the experiments and attempts to extract variations in half-density radius and skin thickness are unreliable because they are so dependent on the assumptions made about the radial shape. The values of $\delta\langle r^2\rangle$ provide a useful test of the validity of effective forces used in nuclear structure calculations. If density independent forces are used, calculations usually result in a shift of the wrong sign (see eg Barrett 1966, Lande *et al* 1968). On the basis of collective models for the motion of the nucleus it is possible to deduce the values of the intrinsic deformation of permanently deformed nuclei or the mean square deformation of vibrational nuclei. Such deformations affect the mean square radius and there have been attempts to separate the contributions to the shift from the change in deformation and the change in 'average' radius. These attempts depend on assumptions about the shape of the radial distribution and they will not be discussed here.

An interesting feature of isotope shifts which has been known for a long time is the 'odd–even staggering effect': in very many cases the shift corresponding to the addition of one neutron to an even-N nucleus is considerably less than half that corresponding to the addition of two neutrons, ie paired neutrons are somehow more effective in increasing the charge radius (see eg Stacey 1966, Reehal and Sorensen 1971). Since paired neutrons tend to go into higher angular momentum states than unpaired ones, the larger radius of these states means that the neutrons attract protons outwards from the central region. Sorenson (1966) has used a collective rather than a single-particle approach and has argued that paired neutrons are more effective in deforming the proton core than unpaired ones (owing to coherence) and that it is the deformation effect which causes odd–even staggering.

From the nuclear structure point of view the subject of isomer shifts is very similar to that of isotope shifts and calculations of the change in mean square radius are sometimes more reliable since there is no change in the number of particles. On the other hand the shifts are much smaller than isotope shifts and the experiments more difficult. There have been optical measurements made on isomers with half lives of a few hours or more (Tomlinson and Stroke 1964). Much shorter-lived excited states have been studied using muonic atoms (Bernow *et al* 1967, 1968,

Baade *et al* 1968a,b, Backe *et al* 1968, Lee *et al* 1972) and in this case the nucleus is excited by the muon itself during its cascade. An analysis of the shifts in ^{207}Pb and ^{209}Bi has been made by Rinker (1971a). An alternative method is that used by Yeboah-Amankwah *et al* (1967) who applied Mössbauer techniques to measure the shift in the transition energy of an atom whose nucleus was the excited daughter nucleus of a radioactive decay. The same technique was used recently by Boolchand *et al* (1972) for isomer shift measurements on ^{182}W, ^{174}Yb, ^{176}Yb, ^{178}Hf and ^{180}Hf.

The general trends in isotope shifts can now be satisfactorily explained in terms of the structure of the nucleus and such effects as the low ratio of the actual to the standard ($A^{1/3}$ rule) shift can be attributed to the deepening of the proton single-particle potential which occurs when neutrons are added (Perey and Schiffer 1966). Explanation of the individual results remains a challenge to nuclear structure theorists.

5.4. Isotone shifts

Experiments which give information about the change in the charge distribution which occurs when a proton is added to a nucleus are of particular value in checking the validity of theoretical calculations. A large number of muonic x ray measurements in the Sn region have been made by Kast *et al* (1971). Their results for the isotone pairs ^{114}Cd–^{115}In, ^{115}In–^{116}Sn, ^{124}Sn–^{126}Te and ^{126}Te–^{127}I are given in table 9

Table 9. Muonic x ray isotone shifts in the tin region

Isotone pair	N	$(\Delta E)_{\text{volume}}/(\Delta E)_{\text{standard}}$[a]
^{114}Cd–^{115}In	66	0·23 (12)[b]
^{115}In–^{116}Sn	66	0·91 (11)[b]
^{120}Sn–^{121}Sb	70	2·8 (9)[c]
^{123}Sb–^{124}Te	72	2·7 (6)[c]
^{124}Sn–^{126}Te	74	1·99 (4)[b]
^{126}Te–^{127}I	74	1·80 (20)[b]

a, the volume shift as calculated in practice is a somewhat model dependent quantity defined by the equation $(\Delta E)_{\text{volume}} = (\Delta E)_{\text{total}} - (\Delta E)_z$ where $(\Delta E)_z$ is defined to be the value which would be obtained for the shift if the heavier isotone had a charge density $\rho(r)$ (normalized to unity) identical with that of the lighter isotone.

b, Kast *et al* 1971

c, Quitman 1967

which also gives the results of measurements of Quitman (1967) for ^{120}Sn–^{121}Sb and ^{123}Sb–^{124}Te. Sinha *et al* (1971) measured electron scattering cross sections for ^{39}K and obtained the difference between the resulting phenomenological density and that from the ^{40}Ca experiment of Frosch *et al* (1968). They compared this difference with the difference obtained from shell model and from Hartree–Fock calculations. Shell model calculations for the isotone pairs ^{15}N–^{16}O, ^{31}P–^{32}S and ^{39}K–^{40}Ca, have also been carried out by Gerace and Hamilton (1972) who adjusted the parameters of the well to give the correct mean square radius in each case. Sick *et al* (1972) have obtained the ^{208}Pb–^{209}Bi difference after measuring the ratio of the electron scattering cross sections and they compare their results with Hartree–Fock calculations. The density differences for ^{39}K–^{40}Ca and ^{208}Pb–^{209}Bi are shown in figures 13 and 14.

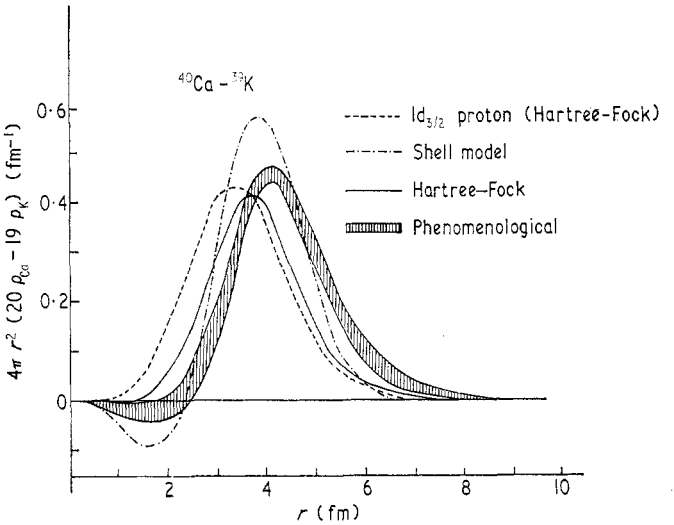

Figure 13. The difference between ^{40}Ca and ^{39}K charge distributions multiplied by $4\pi r^2$ (Sinha *et al* 1971).

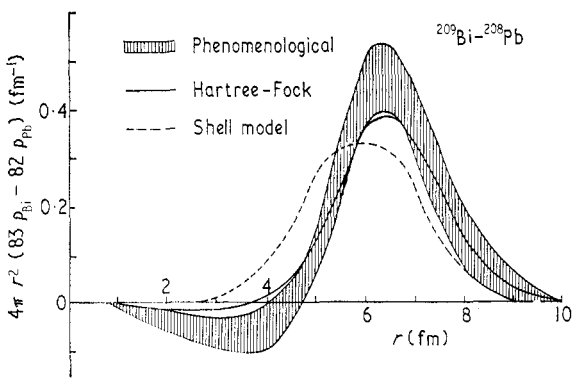

Figure 14. The difference between ^{208}Pb and ^{209}Bi charge distributions multiplied by $4\pi r^2$ (Sick *et al* 1972).

The agreement for ^{208}Pb–^{209}Bi is quite impressive and the effect of the polarization of the core is clearly demonstrated by the negative value of $\Delta\rho$ near the origin. For ^{39}K–^{40}Ca the agreement is not so good partly because the peak of the Hartree–Fock difference comes at too small a radius. It is worth noting once again, however, that even between neighbouring nuclei the model dependence of phenomenological densities may considerably alter the phenomenological differences.

5.5. Deformed nuclei

The intrinsic quadrupole moments of deformed nuclei can be determined (apart from the sign) from B(E2) transition rates and from coulomb excitation cross sections. Results for a large number of nuclei have been compiled by Stelson and Grodzins (1965) and values of the quadrupole deformation parameter β_2 by Stacey (1966). In order to obtain the value of β_2 from the quadrupole moment it is necessary to make an assumption about the radial distribution, and values quoted are often

based on a uniform distribution of radius $R[1+\beta_2 Y_{20}(\theta)]$ which gives

$$Q_0 = \frac{3}{(5\pi)^{1/2}} ZR\beta_2(1+0{\cdot}360\beta_2). \tag{5.2}$$

The value of R is usually taken to be $1{\cdot}2A^{1/3}$ fm. In the analysis of muonic x ray or electron scattering experiments a number of different phenomenological forms have been used, eg the deformed fermi distribution

$$\rho(r,\theta) = \rho_0[e^X+1]^{-1} \tag{5.3}$$

where

$$X = [r-c(1+\beta_2 Y_{20}(\theta))]/a. \tag{5.4}$$

This gives a skin thickness ($t = 4{\cdot}39a$) which is independent of angle. It does have the disadvantage that it is not single-valued at the origin but for heavy nuclei, e^X is so small at $r = 0$ that this is not actually a problem. An alternative form of X is

$$X = [r(1-\beta_2 Y_{20}(\theta))-c]/a \tag{5.5}$$

which gives parallel isodensity contours and a variable skin thickness. An additional parameter has sometimes been used to vary the angular dependence of the skin thickness independently:

$$X = [r-c(1+\beta_2 Y_{20}(\theta))]/Z(1+\beta_2' Y_{20}(\theta)). \tag{5.6}$$

With any of these distributions the quadrupole moment can be calculated by numerical integration:

$$Q = \left(\frac{16\pi}{5}\right)^{1/2} \int_0^\infty \rho(\boldsymbol{r}) Y_{20}(\theta) r^2 \, \mathrm{d}^3 r. \tag{5.7}$$

Some inelastic scattering experiments with α particles have recently demonstrated the existence of Y_{40} (hexadecapole) deformations in nuclei (Hendrie *et al* 1968, Rebel *et al* 1972, Erb *et al* 1972). The Y_{40} deformation in the charge distribution has been obtained from electron inelastic scattering and could in principle be obtained from muonic atom hyperfine spectra. Up until now measurements of the latter have provided the most accurate information about the quadrupole deformation for heavy nuclei although they do not usually give Q_0 directly because of the penetration of the nucleus by the muon wavefunction. If the hyperfine splitting is measured in the 3D state, however, the penetration is small and Q_0 can be determined in a model independent way. Such a measurement has been carried out by Dey *et al* (1973).

In the case of light nuclei the muonic hyperfine splitting is extremely small and electron scattering measurements give deformations much more accurately.

The model dependence of deformed phenomenological densities is even greater because of the additional parameter needed. The parameters which come from phenomenological analyses should therefore be treated with great caution. The more interesting analyses are those in which cross sections or spectra are calculated from theoretically derived deformed densities. An example of how complicated the charge density can be is shown by the isodensity contours in figure 15. The deformation parameters for each contour are given in table 10. The value of β_2 for a uniform distribution with the same quadrupole moment (-20 fm^2) as the density shown in figure 15 is $-0{\cdot}50$.

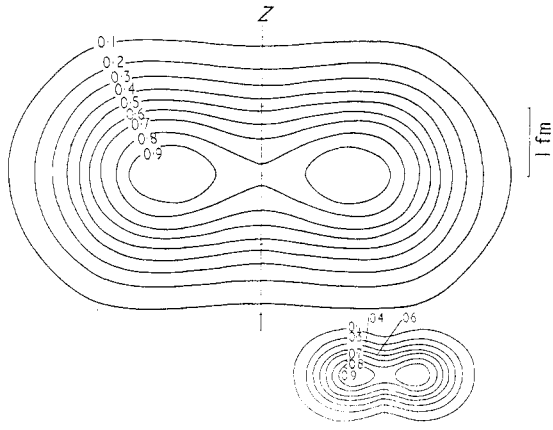

Figure 15. The larger diagram shows isodensity contours for a ^{12}C intrinsic charge distribution obtained from single-particle wavefunctions in a deformed potential (Nilsson model). The resulting cross sections fit the elastic and the inelastic scattering to the 2+ and 4+ states of ^{12}C. The smaller curve is from a Hartree–Fock calculation (Ripka 1968). The figure is taken from Nakada *et al* (1971).

Table 10. Deformation of isodensity contours for ^{12}C

R_0 (fm)	ρ/ρ_{max}	β_2	β_4
1·09	0·8	−2·27	0·73
1·48	0·7	−1·47	0·34
1·71	0·6	−1·22	0·23
1·93	0·5	−1·04	0·15
2·13	0·4	−0·92	0·10
2·36	0·3	−0·82	0·07
2·63	0·2	−0·74	0·04
3·01	0·1	−0·63	0·01
3·33	0·005	−0·59	0·004
3·90	0·001	−0·52	−0·02

The contours are fitted by the function $\acute{R} = R_0(1+\beta_2 Y_{20}+\beta_4 Y_{40})$. The table is reproduced from Nakada *et al* (1971).

Densities obtained from deformed Hartree–Fock calculations have been used for a comparison of calculated and experimental elastic and inelastic form factors by Ripka (1972). Results were obtained for ^{20}Ne, ^{24}Mg and ^{28}Si using both a Negele density dependent force and a Brink and Boeker force in the Hartree–Fock calculations. The fits were moderately good but indicated some shortcomings in the Hartree–Fock wavefunctions.

Table 11 shows the phenomenological parameters and quadrupole moments derived from muonic hyperfine spectra (Hitlin *et al* 1970). The three-parameter deformed fermi distribution which fits the muonic energies predicts quadrupole moments which are in good agreement with those obtained from coulomb excitation measurements. This suggests that in these heavy nuclei the variation of shape of the isodensity contours shown in figure 15 does not occur. (In an earlier analysis, made without corrections for nuclear polarization, Hiltlin *et al* found that the predicted quadrupole moments were too high unless a more complicated form of the density such as expression (5.6) with β' negative were used. The ease with which an error

in the theory was compensated by a change in the phenomenological density should serve as a warning.)

Table 11. Deformation parameters from muonic x ray hyperfine splitting

Nucleus	c	a	β	Q_{OCE}	$Q_{\mathrm{O}\mu}$
^{150}Nd	5·87	0·533	0·278	5·17 (12)	5·15[a]
^{152}Sm	5·90	0·538	0·296	5·85 (15)	5·78[a]
^{162}Dy	6·01	0·547	0·338	7·12 (12)	7·36[a]
^{164}Dy	6·11	0·499	0·334	7·50 (20)	7·42[a]
^{168}Er	6·17	0·497	0·333	7·66 (15)	7·77[a]
^{170}Er	6·27	0·442	0·326	7·45 (13)	7·75[a]
^{182}W	6·41	0·482	0·248	6·58 (6)	6·57[b]
^{184}W	6·42	0·493	0·237	6·21 (6)	6·27[b]
^{186}W	6·46	0·478	0·222	5·93 (05)	5·90[b]

The deformed density used was that given by equations (5.3) and (5.4) and the parameters come from the measurements and calculations of Hitlin *et al* (1970).

a, Stelson and Grodzins 1965

b, Persson and Stokstad 1969

There is a great deal of information about deformed nuclear charge densities and nuclear models which has not been derived up till now but can be obtained in principle from electron scattering and muonic x ray measurements. For example the measurement of very low intensity lines in the hyperfine spectra of muonic atoms, as well as improvements in the accuracy of measurements, will provide information about excited state quadrupole moments, about differential radial moments of the quadrupole charge form factor and information about higher multipole moments. Some of these quantities have been obtained by other means, eg the excited state quadrupole moments by the re-orientation effect in coulomb excitation (de Boer and Eichler 1968) and higher multipole moments by electron and α particle scattering (Bertozzi *et al* 1972, Hendrie *et al* 1968). It is desirable, however, that they should be measured by as many methods as possible.

6. Conclusions

Over the last two or three years our knowledge of charge distributions has increased considerably due to a number of contributing factors: the ever-increasing accuracy of the experiments; the improvements in the calculations which are done to analyse these experiments, particularly in the corrections to the simple picture of an electron or muon moving in a static electric field; the advances in Hartree–Fock calculations and the resulting densities. At the same time it has become apparent that certain deductions about charge densities based on phenomenological distributions are unreliable or misleading, eg values of the half-density radius and 90–10% skin thickness which becomes difficult to define for any but the simplest functional forms, and which depend on the choice of those functional forms. The experiments determine certain integral properties of nuclear charge densities, and measurements of electron scattering, electronic atom and muonic atom levels determine different properties in general. This means that the results of one experiment can be checked only approximately against those of a different type of experiment. When all the available experimental information is combined, then this provides a severe test of densities calculated from Hartree–Fock wavefunctions and

when the test is passed then we can have a certain amount of confidence in the accuracy of the densities. Hartree–Fock calculations have been carried out only for a selected group of nuclei, however, so that we have to use phenomenological densities for other cases. For many purposes this is sufficiently accurate and these densities are useful provided they are treated with sufficient caution. (It is never justified to use a model dependent phenomenological density to obtain such information as the radius at which the density has fallen to 1% of its maximum value.) There is still a need for improvements in the calculations of certain corrections and of Hartree–Fock wavefunctions. Such improved calculations are appearing regularly at this time and soon there will, no doubt, be much more reliable determinations of charge densities.

Acknowledgments

The author is deeply indebted to B. A. Barrett, D. F. Jackson, R. C. Johnson, G. W. Rawitscher, I. Sick and D. W. Stacey for discussions, suggestions and comments on the manuscript, to F. Lenz, G. Ripka, Ciofi degli Atti and M. E. Grypeos for helpful correspondence, and to the large number of people who sent preprints of relevant papers.

Appendix 1. Model independent analysis of elastic scattering cross sections

The delta-shell method of Lenz. The first attempts to obtain model independent analyses of elastic electron scattering were made by Lenz (1968, 1969) and Friedrich and Lenz (1972).† They responded to the need for wider variety in the initial choice of charge distributions by approximating the density by a number of spherical shells and varying the radii and the amount of charge in each of the shells. For their 124 and 167 MeV ^{208}Pb data they found that about 10 shells were sufficient to reproduce the cross sections. Examples of their distributions are shown in figure 16. As a test of the spherical shell approximation they reproduced the theoretical cross section due to a typical continuous charge density with a value of χ^2 (the weighted mean square deviation) of as little as 0·007. The best value of χ^2 for real experimental points was about 0·77.

The spherical shell density distribution may be written as follows:

$$\rho_\delta(r) = \sum_{i=1}^{N} p_i \, \delta(r - R_i)/R_i^2. \tag{A.1}$$

At the beginning of a calculation their 'functional form' was chosen by fixing the values of p_i and N, and the shell radii R_i were then varied to give the best fit to the cross section (the radii R_i were allowed to cross each other). During the variations they used the distorted wave born approximation DWBA to obtain the variations in the phase shifts, but after a number of iterations they would solve the Dirac equation again for the new density distribution. Their method enabled them to do

† Model independence has been claimed for a different method of analysis (Luk'yanov *et al* 1969, Pol 1969), which is based on a linear combination of derivatives of the fermi distribution. Although this is more general than the the usual phenomenological densities, the terms are not orthogonal in the sense described later in this appendix. If the number of terms is small enough to prevent the uncertainties in the density from being unreasonably large, the method becomes model dependent.

thousands of calculations and they were able to find densities derived from hundreds of different 'functional forms' which gave good fits to the cross sections.

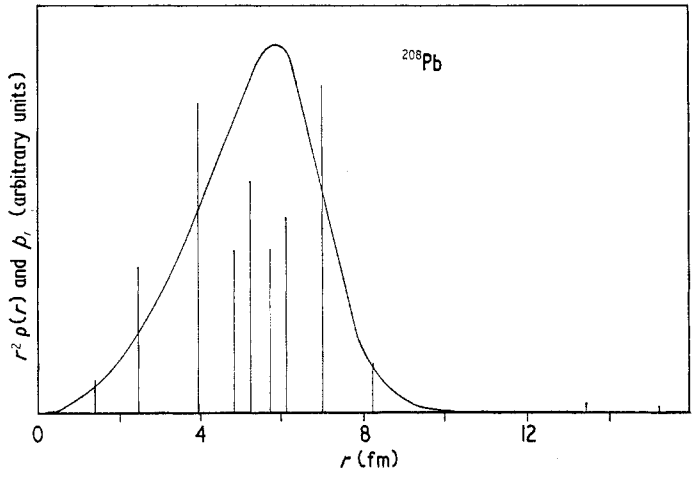

Figure 16. The continuous curve corresponds to a fermi distribution and the vertical lines represent a series of spherical shells each containing an amount of charge proportional to the height. The spherical shell distribution is one of many hundreds which have been found to give a good fit to the 124 and 167 MeV electron scattering on ^{208}Pb (Friedrich and Lenz 1972).

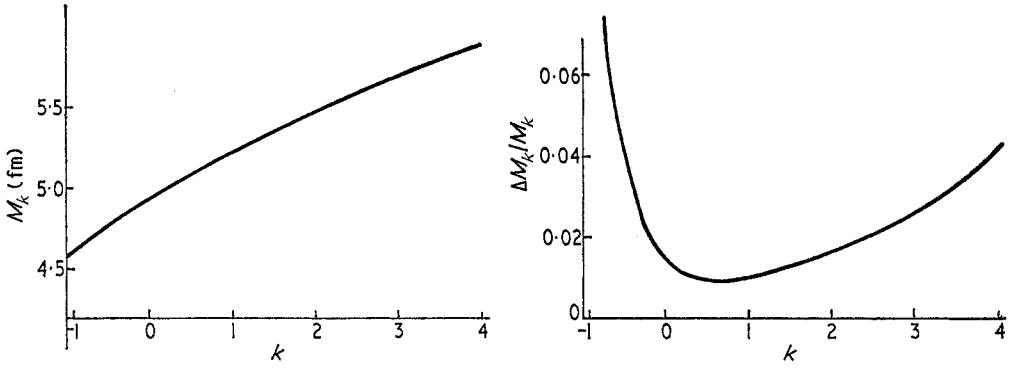

Figure 17. The lefthand curve shows an average (over all the δ shell charge distributions which fit the scattering) of the moment M_k plotted against k. The righthand curve shows values of $\Delta M_k/M_k$ where ΔM_k is the spread in M_k over the different distributions (Friedrich and Lenz 1972).

Using all these different density distributions Friedrich and Lenz calculated two different integral properties of the charge distribution. One of them was the moment M_k which, apart from a trivial factor, is the same as the equivalent uniform radius R_k of Ford and Wills (1969):

$$M_k = \left(\frac{k+3}{3}\right)^{1/k} R_k = \left[\int \rho(r)\, r^k \, \mathrm{d}^3 r\right]^{1/k}. \qquad \text{(A.2)}$$

The values of M_k averaged over all the charge distributions, together with the error or spread in M_k, are plotted as functions of k in figure 17. The interesting feature in

the error curve is the minimum at about $k = 0{\cdot}5$ where the error is about 1%. The error is less than 2% over the range $-0{\cdot}2 < k < 2$. These errors should be treated as lower limits if we want to claim that they are determined by the cross sections and do not contain any preconceived ideas about the charge distribution, since we know very little about the extremely low density region and yet a small amount of charge in this region contributes a large amount to the higher moments. If we go out far enough from the centre of the nucleus then the only observable effect on the cross sections of adding a small amount of charge is to change the magnitude and not the angular shape. An extreme example of this was given by Barrett *et al* (1968), who examined the electron–proton scattering data and decided that, *on the basis of the experimental cross sections alone*, it was impossible to say what the mean square radius of the proton was to within a factor of 3 or more.

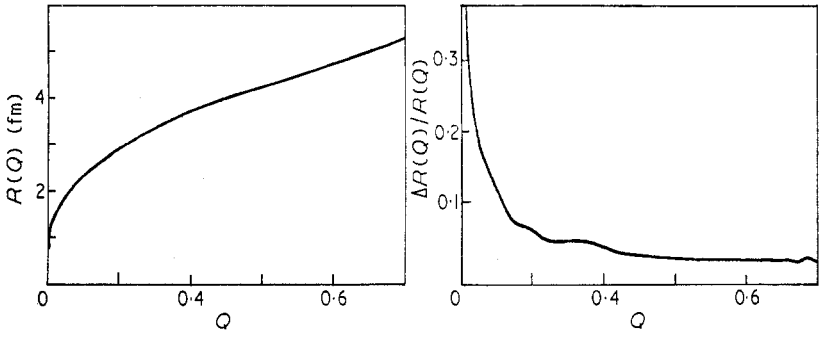

Figure 18. The curve on the left shows an average (over δ shell distributions) of the mean radius $R(Q)$, of the innermost Qth fraction of the charge density plotted against Q. The curve on the right shows values of $\Delta R(Q)/R(Q)$ where $\Delta R(Q)$ is the spread in $R(Q)$ over the different distributions (Friedrich and Lenz 1972).

The other quantity which Friedrich and Lenz calculated for all their charge distributions was the average radius $R(Q)$ of the innermost fraction Q of the total charge, ie

$$R(Q) = \frac{4\pi}{Q}\int_0^a \rho(r) r^3 \, dr \tag{A.3}$$

where a is the radius of the sphere which contains a fraction Q of the charge:

$$Q(a) = 4\pi \int_0^a \rho(r) r^2 \, dr. \tag{A.4}$$

If we know the function $R(Q)$ then we can calculate $\rho(r)$ from the equations

$$\frac{d}{dQ}(Q(a)\, R(Q)) = a \tag{A.5}$$

$$\rho(a) = \left(4\pi a^2 \frac{da}{dQ}\right)^{-1}. \tag{A.6}$$

The average values of $R(Q)$ together with the error or spread in $R(Q)$ for the 640 spherical shell distributions which fitted the 124 and 167 MeV data are shown as functions of Q in figure 18. This shows how the error in $R(Q)$ falls very rapidly in the region $0 < Q < 0{\cdot}2$ to a value which then remains almost constant in the region of 3–5%.

Friedrich and Lenz then produced a number of continuous distributions in an unusual way, namely by inventing functional forms for $R(Q)$ and fitting them to the curve in figure 18. Equations (A.5) and (A.6) then enabled them to produce the densities and some of the results are shown in figures 11 and 19. These very striking curves indicate how far it is possible to go from the previously assumed shapes of the charge distribution and still fit the data.

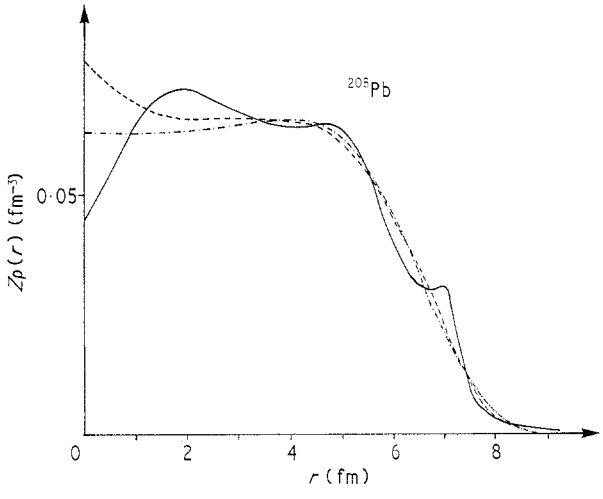

Figure 19. Charge densities for ^{208}Pb which give good fits to the 124 and 167 MeV elastic electron scattering cross sections.

The method of Friar and Negele. An alternative method of obtaining model independent charge distributions is to expand the density in terms of a complete set of functions. The success of the method depends crucially on the choice of the set: they should be chosen to be orthogonal in the sense that the contributions of the different functions to the experimentally measured quantities are, as far as possible, independent, eg each function should contribute to the electron scattering cross section only for a small range of q values. Friar and Negele (1973) have made an exhaustive study of ^{208}Pb using this method. They represent the function $r\rho(r)$ by a Fourier sine series, whose terms are orthogonal (in the above sense) for electron scattering cross sections analysed in the (plane wave) Born approximation. (However, they do no do their calculations in the plane wave Born approximation.) They use muonic x ray energies as well as electron scattering cross sections to determine the coefficients of the Fourier series.

In practice Friar and Negele proceed as follows: they assume an initial density $\rho_0(r)$ which gives a reasonable fit to experiment and calculate electron and muon wavefunctions. They then use the distorted wave Born approximation (or first order perturbation theory) to calculate the effect of a small change $\delta\rho$ on the experimentally determined quantities. Expanding $\delta\rho$ as

$$\delta\rho = \frac{1}{r}\sum_{N=1}^{L} C_N \sin\left(\frac{N\pi r}{R}\right)$$

they are able to predict the values of the coefficients C_N which give the best fit to experiment. The density is assumed to be zero for $r > R$ and the value of R chosen

to be 11 fm (although the results are insensitive to changes in R over the range $11 < R < 15$ fm). The number of terms L is chosen so that $\delta\rho$ contributes to the form factor only for $q < q_{\max}$ where $q_{\max}$ is the maximum measured momentum transfer. The procedure can be iterated, using $\rho_0^{(i)} + \delta\rho^{(i)} = \rho_0^{(i+1)}$. This method gives not only the best fit to experiment but also the error matrix for the coefficients C_i. The correlation of the errors in the charge density,

$$f(r,r') = \overline{[\rho(r) - \overline{\rho(r)}]\,[\rho(r') - \overline{\rho(r')}]}$$

can be calculated in terms of the error matrix and the RMS error in the density is

$$\Delta\rho = [f(r,r)]^{1/2}.$$

A value of the error for quantities of the form

$$\langle G \rangle = \int^{\infty} g(r)\,\rho(r)\,r^2\,\mathrm{d}r$$

is also easily obtainable. These errors depend on the assumption that the experimental errors are purely statistical.

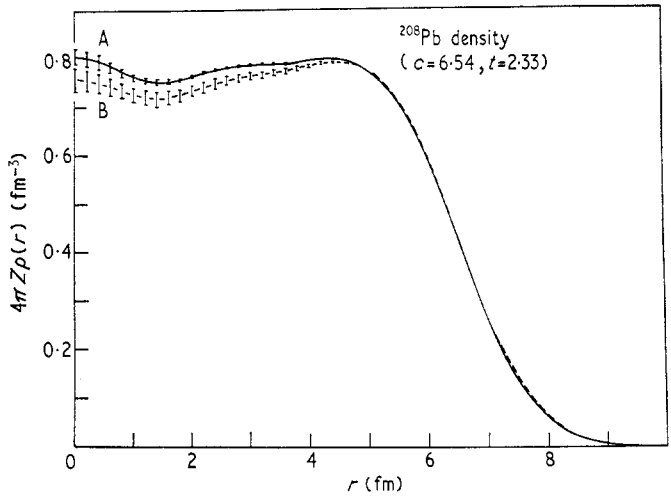

Figure 20. The charge density of ^{208}Pb from the model independent analysis of Friar and Negele (1973). The full curve comes from the simultaneous analysis of muonic x ray and electron scattering data and the broken curve from electron scattering alone. The vertical bars represent the statistical errors in the density.

Like all other methods this cannot, of course, give any information on the existence of high frequency oscillations in the density, corresponding to momentum transfers beyond the range of experimental information. Thus the envelope formed by the curves $\rho(r) \pm \Delta\rho(r)$ gives the limits of the density subject to the possibility that they may be exceeded by such an oscillation. If $q_{\max}$ is sufficiently large then we may rule out the possibility of substantial high frequency oscillations on theoretical grounds due to the finite size and the maximum binding energy of the proton.

Two densities obtained by Friar and Negele are shown together with their statistical errors in figure 20. The full curve is the result of a simultaneous fit to electron scattering and muonic x ray data and the broken curve was obtained fitting electron scattering only. The fact that the error in each curve does not overlap the

other indicates that the experimental errors are not purely statistical. The discrepancy would be removed by a change in normalization of the electron scattering cross section by 2 or 3%. Friar and Negele have suggested that there may indeed be such an error due to the neglect of vacuum polarization in the electron scattering analysis.

Borysowicz and Hetherington (1973) have also expanded the density in a series of functions and applied the method to ^{3}He and ^{4}He. They used cosine functions and spline functions and obtained densities and errors on the densities in a similar way.

Appendix 2. Model independent analysis of muonic x ray spectra

The aim of this analysis is to find what there is in common between different charge distributions which give the same x ray spectrum (within experimental error). The necessity for doing this is demonstrated by the densities in figure 21

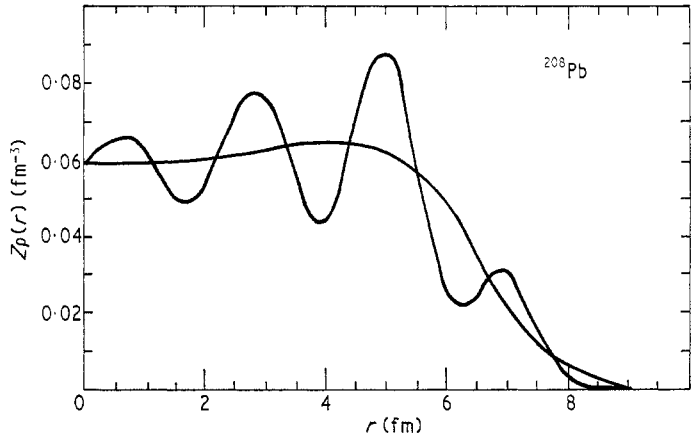

Figure 21. Charge densities which give muonic x ray energies consistent with the experimental values (Ford and Rinker 1972).

which both fit the experiments (Ford and Rinker 1972). This was done previously for optical isotope shifts and low energy (and low Z) electron scattering, with the result that charge distributions which fitted the experiments had the same mean square radius. In first order perturbation theory a change $\Delta\rho(r)$ in the charge distribution results in the following change in the energy E_j of a state j:

$$\Delta E_j = -Ze^2 \int\int \frac{\psi_j^+(\boldsymbol{r}')\psi_j(r')\Delta\rho(r)\,\mathrm{d}^3r\,\mathrm{d}^3r'}{|\boldsymbol{r}-\boldsymbol{r}'|} \tag{B.1}$$

$$\equiv -Ze^2 \int f_j(r)\Delta\rho(r)r^2\,\mathrm{d}r \tag{B.2}$$

where

$$f_j(r) = \int \frac{\psi_j^+(\boldsymbol{r}')\psi_j(\boldsymbol{r}')}{|\boldsymbol{r}-\boldsymbol{r}'|}\mathrm{d}^3r'\,\mathrm{d}\Omega \tag{B.3}$$

is the spherically averaged charge distribution due to the 'muon cloud'. Thus a

small change $\Delta\rho$ will not change the binding energy E_j if

$$\int f_j(r)\,\Delta\rho(r)\,r^2\,\mathrm{d}r = 0. \tag{B.4}$$

Alternatively we can say that a measurement of E_j determines the quantity

$$\langle f_j\rangle = \int f_j\,\rho(r)\,r^2\,\mathrm{d}r. \tag{B.5}$$

(Obviously f_j is not independent of $\rho(r)$ but it varies very slowly with ρ especially if the latter is constrained to give the right transition energies.) In practice we measure energy differences and the transition energy E_{ij} between states i and j therefore gives us the quantity

$$\langle f_{ij}\rangle \equiv \int (f_i - f_j)\,\rho(r)\,r^2\,\mathrm{d}r. \tag{B.6}$$

We can expand $f_{ij}(r)$ in a series

$$f_{ij} = \sum_{n=0}^{\infty} a_n r^{2n} \tag{B.7}$$

and thus obtain the dependence of E_{ij} on even moments of the charge density. This has been done by Bethe and Negele (1968). In practice this does not work well for medium and heavy nuclei; for a finite polynomial fit to f_{ij}, the coefficients of the lowest terms vary drastically as the order of the polynomial changes. Bethe and Negele tried to overcome this difficulty by expanding f_{ij} about the nuclear surface. Their method is rather cumbersome to use, however, and requires the tabulation of a large number of coefficients.

The method of Ford and Wills (1969) is essentially a way of approximating the function f_{ij} by the formula

$$f_{ij} \simeq a + br^k. \tag{B.8}$$

Their functions were of such a form that they varied only near the nuclear surface, however, so that they automatically chose a, b and k to fit f_{ij} in this region. In many transitions this means that the fit to f_{ij} is not a good approximation over the whole nuclear region. A better approximation can obviously be obtained by using a more general function. Although this makes the interpretation more complicated and is not so aesthetically pleasing as the single fractional moment of Ford and Wills, it is nevertheless necessary for the lowest transitions. Barrett (1970) found that the function $a + br^k\,\mathrm{e}^{-\alpha r}$ with one additional parameter α gave a very much better fit to f_{ij} and approached the ideal of model independence for almost all transitions.

The additional parameter needed to achieve this makes the systematic study of muonic x ray results much more complicated. Fortunately a reasonable fit to all the functions f_{ij} for a particular nucleus can be obtained with the parameter α fixed and only a, b and k varying for the different transitions. This method has been used by Ford and Rinker (1972) in a very comprehensive study of lead isotopes. A plot of their results for ^{208}Pb is shown figure 12. The quantity R_k is defined to be the radius of the uniform charge distribution which has a generalized moment $\langle r^k\,\mathrm{e}^{-\alpha r}\rangle$ whose value is either determined by experiment or is the same as a phenomenological distribution. The accuracy to which a generalized moment can be obtained (for a given experimental error in the corresponding transition) depends on the

value of the expectation value $\langle \Delta V \rangle$ where

$$\Delta V = V(r) - V_{\text{point}}(r).$$

Values of $\langle \Delta V \rangle$ for different muon states are plotted against Z in figure 22.

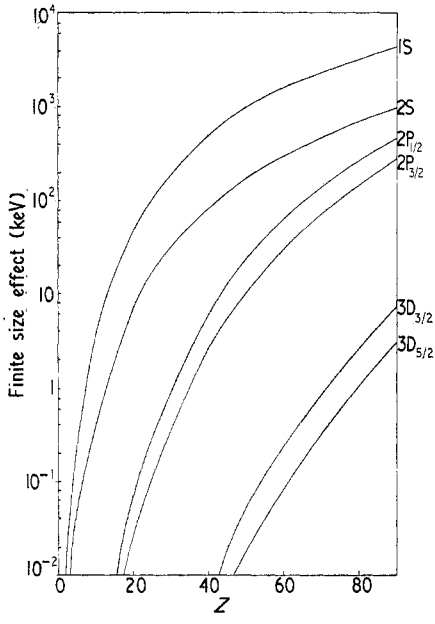

Figure 22. The nuclear finite size effect in muonic atoms for different levels.

References

AKHIEZER A I and BERESTETSKII V B 1965 *Quantum Electrodynamics*, trans. G M Volkoff (New York: Interscience) p703

ANDERSON H L, HARGROVE C K, HINCKS E P, MCANDREW J D, MCKEE R J, BARTON R D and KESSLER D 1969 *Phys. Rev.* **187** 1565–96

BAADE R, BACKER H, ENGFER R, HESSE K, KANKELEIT E, SCHRÖDER U, WALTER H K and WIEN K 1968a *Phys. Lett.* **27B** 425–7

—— 1968b *Phys. Lett.* **27B** 428–30

BACKE H, BACKENSTOSS G, DANIEL H, ENGFER R, KANKELEIT E, POELZ G, SCHMITT H, TANSCHER L and WIEN K 1968 *Hyperfine Structure and Nuclear Radiations* (Amsterdam: North-Holland) pp65–70

BACKENSTOSS G *et al* 1973 to be published

BARDIN T T, COHEN R C, DEVONS S, HITLIN D, MACAGNO E, RAINWATER J, RUNGE K, WU C S and BARRETT R C 1967 *Phys. Rev.* **160** 1043–54

BARREAU P and BELLICARD J B 1967 *Phys. Lett.* **25B** 470–2

BARRETT R C 1966 *Nucl. Phys.* **88** 128–35

—— 1967 *Proc. Int. Conf. on Electromagnetic Sizes of Nuclei* ed D J Brown, M K Sundaresan and R D Barton (Ottawa: Carleton University) pp134–42

—— 1968 *Phys. Lett.* **28B** 93–5

—— 1969 *Proc. Int. Conf. on Properties of Nuclear States* ed M Harvey, J Y Cusson, J S Geiger and J M Pearson (Montreal: Université de Montréal) pp109–23

—— 1970 *Phys. Lett.* **33B** 388–94

BARRETT R C, BRODSKY S J, ERICKSON G W and GOLDHABER M H 1968 *Phys. Rev.* **166** 1589–98

BARRETT R C, OWEN D A, CALMET J and GROTCH H 1973 to be published

BAUCHE J 1966 *C. R. Acad. Sci., Paris* **B263** 685–8
—— 1969 *PhD Thesis* Orsay
BELLICARD J B, BOUNIN P, FROSCH R F, HOFSTADTER R, MCCARTHY J S, URHANE F J, YEARIAN M R, CLARK B C, HERMAN R and RAVENHALL D G 1967 *Phys. Rev. Lett.* **19** 527–9
—— 1968 *Phys. Rev. Lett.* **20** 977
BENTZ H A 1969 *Z. Naturforsch.* **A24** 858–9
BERNOW S, DEVONS S, DUERDOTH I, HITLIN D, KAST J W, LEE W Y, MACAGNO E R, RAINWATER J and WU C S 1968 *Phys. Rev. Lett.* **21** 457–61
BERNOW S, DEVONS S, DUERDOTH I, HITLIN D, KAST J W, MACAGNO E R, RAINWATER J, RUNGE K and WU C S 1967 *Phys. Rev. Lett.* **18**, 787–90
BERTOZZI W, COOPER T, ENSSLIN N, HEISENBERG J, KOWALSKI S, MILLS M, TURCHINETZ W, WILLIAMSON C, FIVOZINSKY S P, LIGHTBODY J W and PENNER S 1972 *Phys. Lett Rev.* **28** 1711–3
BERTOZZI W, FRIAR J, HEISENBERG J and NEGELE J W 1972 *Phys. Lett.* **41B** 408–4
BETHE H A 1968 *Phys. Rev.* **167** 879–907
—— 1971 *Ann. Rev. Nucl. Sci.* **21** 93–244
BETHE H A and MOLINARI A 1971 *Ann. Phys.* **63** 393–431
BETHE H A and NEGELE J W 1968 *Nucl. Phys.* **117A** 575–85
BETHE H A and SALPETER E E 1957 *Quantum Mechanics of One- and Two-Electron Atoms* (Berlin: Springer-Verlag) p195
BHATTACHERJEE S K, BOEHM F and LEE P L 1969 *Phys. Rev.* **188** 1919–29
BISHOP G R 1965 in *Nuclear Structure and Electromagnetic Interactions* ed N MacDonald (New York: Plenum) p211
BLATT J M and WEISSKOPF V F 1952 *Theoretical Nuclear Physics* (New York: John Wiley) pp565–82
BODMER A R 1953 *Proc. Phys. Soc.* **A66** 1041–58
—— 1959 *Nucl. Phys.* **9** 371–99
BOEHM F 1972 *Proc. Int. Conf. on Inner Shell Ionization Phenomena, Atlanta, U.S.A., April* 17–22
BOEHM F and LEE P L 1972 to be published
BOHR A and MOTTELSON B R 1953 *Mat. Fys. Medd. Dan. Vid. Selsk* **27** No 16
BOHR N 1922 *Nature, Lond.* **109** 746
BOOLCHAND P, LANGHAMMER D, CHING-LU LIN and JHA S 1972 *Phys. Rev.* **C6** 1093–8
BORYSOWICZ J and HETHERINGTON J 1973 to be published
BREIT G 1958 *Rev. Mod. Phys.* **30** 507–16
BRIX P and KOPFERMANN H 1949 *Z. Phys.* **126** 344–64
—— 1958 *Rev. Mod. Phys.* **30** 517–20
BROWN G E 1970 *Facets of Physics* ed D A Bromley and V W Hughes (New York and London: Academic Press) pp141–50
—— 1971, *Unified Theory of Nuclear Models and Forces* 3rd edn (Amsterdam: North-Holland)
BROWN G E and ELTON L R B 1955 *Phil. Mag.* **46** 164–76
BRUECKNER K A, MELDNER H W and PEREZ J D 1972 *Phys. Rev.* **C6** 773–9
BUDINI P and FURLAN G 1959 *Nuovo Cim.* **13** 790–801
BURHOP E H S 1969 *High Energy Physics* (New York: Academic Press) vol 3 pp109–281
CAMPI X, MARTORELL J and SPRUNG D W L 1972 *Phys. Lett.* **41B** 443–5
CAMPI X and SPRUNG D W 1972 *Nucl. Phys.* **A194** 401–42
CHEN M Y 1968 *PhD Thesis* Princeton University
—— 1970a *Phys. Rev.* **C1** 1167–75
—— 1970b *Phys. Rev.* **C1** 1176–83
CHESLER R B 1967 *PhD Thesis* California Institute of Technology
CHESLER R B and BOEHM F 1968 *Phys. Rev.* **166** 1206–12
CIOFI DEGLI ATTI C 1969 *Nucl. Phys.* **A129** 350–68
—— 1971 *Phys. Rev.* **C4** 1473–5
CIOFI DEGLI ATTI C and KABACHNIK N M 1970 *Phys. Rev.* **C1** 809–15
CIOFI DEGLI ATTI C, LANTTO L and TOROPAINEN P 1972 *Phys. Lett.* **42B** 27–30
COHEN S 1960 *Phys. Rev.* **118** 489–94
COLE R K JR 1969 *Phys. Rev.* **177** 164–83
CZYŻ W and LEŚNIAK L 1967 *Phys. Lett.* **25B** 319–21

DALITZ R H 1951 *Proc. Roy. Soc. A* **206** 509–20
DE BOER J and EICHLER J 1968 *Advances in Nucl. Phys.* **1** 1–65
DE FOREST T 1967 *Ann. Phys.* **45** 365–403
DE FOREST T and WALECKA J D 1966 *Advan. Phys.* **15** 1–111
DE JAGER C W, MASS R and DE VRIES C 1972 *Phys. Lett.* **39B** 188–90
DEVONS S and DUERDOTH I 1969 *Adv. Nucl. Phys.* **2** 295–423
DEY W, EBERSELD P, LEISI H J and SCHECK F 1972 *Proc. Int. Conf. on Nuclear Moments and Nuclear Structure, Osaka, Japan, September* 4–8
DIRAC P A M 1958 *The Principles of Quantum Mechanics* (Oxford: Clarendon Press)
DIXIT M S, ANDERSON H L, HARGROVE C K, MCKEE R J, KESSLER D, MES H and THOMPSON A C 1971 *Phys. Lett.* **27** 878–80
DONNELLY T W and WALKER G E 1969 *Phys. Rev. Lett.* **21** 1121–4
DOWNS B W, RAVENHALL D G and YENNIE D R 1957 *Phys. Rev.* **106** 1285–9
DREHER B, LEMB M and LENZ F 1972 to be published
EHRENBERG H F, HOFSTADTER R, MEYER-BERKHOUT U, RAVENHALL D G and SOBOTTKA S E 1959 *Phys. Rev.* **113** 666–000
EHRENFEST P 1922 *Nature, Lond.* **109** 745–6
EHRLICH R D 1968 *Phys. Rev.* **173** 1088–100
EHRLICH R D, FRYBERGER D, JENSEN D A, NISSIM-SABAT C, POWERS R J, TELEGDI V L and HARGROVE C K 1967 *Phys. Rev. Lett.* **19** 959–65
EISENSTEIN R A, MADSEN D W, THEISSEN H, CARDMAN L W and BECKELMAN C K 1969 *Phys. Rev.* **188** 1815–30
ELTON L R B 1950 *Proc. Phys. Soc.* **A63** 1115–24
—— 1961, *Nuclear Sizes* (Oxford: Clarendon Press)
—— 1967a *Proc. Int. Conf. on Electromagnetic Sizes of Nuclei* ed D J Browne, M K Sundaresan and R D Barton (Ottawa: Carleton University) pp267–98
—— 1967b *Landolt–Börnstein: Numerical Data and Functional Relationships in Science and Technology* vol 2 ed H Schopper (Berlin: Springer-Verlag) pp1–20
ELTON L R B and SWIFT A 1967 *Nucl. Phys.* **A94** 52–72
ELTON L R B and WEBB S J 1970 *Phys. Rev. Lett.* **24** 145–8
ELTON L R B, WEBB S J and BARRETT R C 1969 *Proc. Third Int. Conf. on High Energy Physics and Nuclear Structure* (New York: Plenum Press) pp67–73
ERB K A, HOLDEN J E, LEE I Y, SALADIN J X and SAYLOR T K 1972 *Phys. Rev. Lett.* **29** 1010–4
ERNST D J, SHAKIN C M and THALER R M 1973 *Phys. Rev.* **C7** 925–30
FAESSLER A, GALONSKA J E and GOEKE K 1972 *Z. Phys.* **250** 436–45
FAJARDO L A, FICENEC J R, TROWER W P and SICK I 1971 *Phys. Lett.* **37B** 363–5
FICENEC J R, FAJARDO L A, TROWER W P and SICK I 1972 *Phys. Lett.* **42B** 213–5
FINK M, HEBACH H and KUMMEL H 1971 *Phys. Rev.* **C3** 2075–6
FITCH V L and RAINWATER J 1953 *Phys. Rev.* **92** 789–800
FORD K W 1972 *Magic Without Magic: John Archibald Wheeler* ed J Klauder (New York: Freeman)
FORD K W and RINKER G A JR 1973 *Phys. Rev.* **C7** 1206–21
FORD K W and WILLS J G 1969 *Phys. Rev.* **185** 1429–38
FOSTER E W 1951 *Rep. Prog. Phys.* **14** 288–315
FRIAR J L 1971 *Nucl. Phys.* **A173** 257–64
FRIAR J L and NEGELE J W 1973 to be published
FRIAR J L and ROSEN M 1972 *Phys. Lett.* **39B** 615–9
FRIEDRICH J. and LENZ F 1972 *Nucl. Phys.* **A183** 523–44
FROSCH R F 1971 *Phys. Lett.* **37B** 140–2
FROSCH R F, HOFSTADTER R, MCCARTHY J S, NÖLDEKE G K, VAN OOSTRUM K J, YEARIAN M R, CLARK B C, HERMAN R and RAVENHALL D G 1968 *Phys. Rev.* **174** 1380–99
FROSCH R F, MCCARTHY J S, RAND R E and YEARIAN M R 1967 *Phys. Rev.* **160** 874–9
GAMOW G 1928 *Z. Physik* **52** 510
GAUDIN M, GILLESPIE J and RIPKA G 1971 *Nucl. Phys.* **A176** 237–60
GERACE W J and HAMILTON G C 1972 *Phys. Lett.* **39B** 481–4
GERACE W J and SPARROW D A 1969 *Phys. Lett.* **30B** 71–4
GERSTENKORN S and HELBERT J 1968 *Compt. Rend.* **266** Series B 546–9
GOBLE A T and SILVER J D 1973 to be published

GORODKOV S S and NEMIROVSKII P E 1968 *Yad. Fiz.* **10** 275–80 (English translation: 1970 *Sov. J. Nucl. Phys.* **10** 158–61)
GROTCH H and YENNIE D R 1969 *Rev. Mod. Phys.* **41** 350–74
GRYPEOS M E 1969 *Phys. Rev. Lett.* **23** 793–6
GUTH E 1934 *Anz. Akad. Wiss. Wien, Math.-Naturw. Kl.* **24** 299
HEILIG K, SCHMITZ K and STEUDEL A 1963 *Z. Phys.* **176** 120–5
HEISENBERG J, HOFSTADTER R, MCCARTHY J S, SICK I, CLARK B C, HERMAN R and RAVENHALL D G 1969a *Phys. Rev. Lett.* **23** 1402–5
—— 1969b *Proc. Third Int. Conf. on High Energy Physics and Nuclear Structure* (New York: Plenum Press) pp33–9
HEISENBERG J, HOFSTADTER R, MCCARTHY J S, SICK I, YEARIAN M R, CLARK B C, HERMAN R, RAVENHALL D G 1971a *Topics in Modern Physics* ed W E Brittin and H Odabasi (London: Adam Hilger) pp169–90
HEISENBERG J H, MCCARTHY J S, SICK I and YEARIAN M R 1971b *Nucl. Phys.* **A164** 340–52
HENDRIE D L, GLENDENNING N K, HARVEY B G, JARVIS Q N, DUHM H H, SANDINOS J and MAHONEY J 1968 *Phys. Lett.* **26B** 127–30
HILL D L and FORD K W 1954 *Phys. Rev.* **94** 1616–29
HITLIN D, BERNOW S, DEVONS S, DUERDOTH I, KAST J W, MACAGNO E R, RAINWATER J, WU C S and BARRETT R C 1970 *Phys. Rev.* **C1** 1184–201
HOFSTADTER R 1956 *Rev. Mod. Phys.* **28** 214–54
—— 1957 *Ann. Rev. Nucl. Sci.* **7** 231–316
HOFSTADTER R and COLLARD H R 1967 *Landolt–Börnstein: Numerical Data and Functional Relationships in Science and Technology* vol 2 ed H Schopper (Berlin: Springer-Verlag) pp21–64
HUBBARD L B, MCGRORY J B and JOLLY H P 1972 *Phys. Rev.* **C6** 532–6
HUGHES D J and ECKART D 1930 *Phys. Rev.* **36** 694–8
INOPIN E V 1971 *Proc. Fourth Int. Conf. on High Energy Physics and Nuclear Structure, Dubna, September* 6–11 1971
JACKSON D F 1974 *Rep. Prog. Phys.* **37** 55–146
JACOBSOHN B A 1954 *Phys. Rev.* **96** 1637–43
JANSEN J A, PEERDEMAN R TH and DE VRIES C 1972 *Nucl. Phys.* **A188** 337–52
JENKINS D A, POWERS R J, MARTIN P, MILLER G H and WELSH R E 1971 *Nuc. Phys.* **A175** 73–100
JONES G A 1970 *Rep. Prog. Phys.* **33** 645–89
KAST J W, BERNOW S, CHENG S C, HITLIN D, LEE W Y, MACAGNO E R, RUSHTON A M and WU C S 1971 *Nucl. Phys.* A **169** 62–70
KESSLER D 1971 Carleton University preprint of a paper presented at *Muon Physics Conf., Fort Collins, Colorado, September* 6–10, 1971 (Proceedings ed P Chand to be published by Dekker, New York)
KHANNA F C 1968 *Phys. Rev. Lett.* **20** 871–3
—— 1971 *Nucl. Phys.* **A165** 475–96
KIM Y N 1971 *Mesic Atoms and Nuclear Structure* (Amsterdam: North-Holland)
KING W H 1963 *J. Opt. Soc. Amer.* **53** 638–9
—— 1964 *Proc. Roy. Soc.* A **280** 430–8
—— 1971 *J. Phys.* B **4** 288–95
KUHN H G 1969 *Atomic Spectra* 2nd edn (London: Longmans Green) pp369–85
LAMB W E and RETHERFORD R C 1947 *Phys. Rev.* **72** 241–3
LANDAU L 1944 *J. Phys. U.S.S.R.* **8** 201
LANDE A, MOLINARI A and BROWN G E 1968 *Nucl. Phys.* **A115** 241–52
LEE W Y, CHEN M Y, CHENG S C, MACAGNO E R, RUSHTON A M and WU C S 1972 *Nucl. Phys.* **A180** 14–24
LENZ F 1968 *Diplomarbeit* (unpublished)
—— 1969 *Z. Phys.* **222** 491–503
LENZ F and ROSENFELDER R 1971 *Nucl. Phys.* **A176** 513–25
LIN W-F 1972 *Phys. Lett.* **39B** 447–9
LIPKIN H J 1958 *Phys. Rev.* **110** 1395–403
LITVINENKO A S, SHEVCHENKO N G, BUKI A YU, SAVITSKY G A, KHRASTUNOV V M, KHORMICH A A, POLISHCHUK V N and CHKALOV I I 1972 *Nucl. Phys.* **A182** 265–71

LOMBARD R J 1970 *Phys. Lett.* **32B** 652–5
—— 1972 preprint of review article
LUK'YANOV V K, PETKOV I ZH and POL YU S 1969 *Yad. Fiz.* **9** 349–56 (English translation: 1969 *Sov. J. Nucl. Phys.* **9** 204–7)
LYMAN E M, HANSON A O and SCOTT M B 1951 *Phys. Rev.* **84** 626–34
MACAGNO E R 1968 *PhD Thesis* Columbia University, New York
MACAGNO E R, BERNOW S, CHENG S C, DEVONS S, DUERDOTH I, HITLIN D, KAST J W, LEE W Y, RAINWATER J, WU C S and BARRETT R C 1970 *Phys. Rev.* **C1** 1202–21
MACDONALD L J and ÜBERALL H 1970 *Phys. Rev.* **C1** 2156–7
MCKEE R J 1969 *Phys. Rev.* **180** 1139–58
MCKINLEY H M 1969 *Phys. Rev.* **183** 106–11
MCKINLEY W A and FESHBACH H 1948 *Phys. Rev.* **74** 1759–63
MADSEN D W, CARDMAN L S, LEGG J R and BOCKELMAN C K 1971 *Nucl. Phys.* **A168** 97–128
MARTIN P, MILLER G H, WELSH R E, JENKINS D A, POWERS R J and KUNSELMAN A R 1973 to be published
MAXIMON L C 1969 *Rev. Mod. Phys.* **41** 193–204
MERTON T R 1919 *Proc. Roy. Soc.* A **96** 388–95
MEYER-BERKHOUT U, FORD K W and GREEN A E S 1959 *Ann. Phys. N.Y.* **8** 119–71
MO L W and TSAI Y S 1969 *Rev. Mod. Phys.* **41** 205–35
MOTT N F 1929 *Proc. Roy. Soc.* A **124** 425–42
NAKADA A, TORIZUKA Y and HORIKAWA Y 1971 *Phys. Rev. Lett.* **27** 745–8
NEGELE J W 1970 *Phys. Rev.* **C1** 1260–1320
—— 1971 *Phys. Rev. Lett.* **27** 1291–3
NÉMETH J and RIPKA G 1972 *Nucl. Phys.* **A194** 329–52
ONLEY D S 1968 *Nucl. Phys.* **A118** 436–48
PEREY F G and SCHIFFER J P 1966 *Phys. Rev. Lett.* **17** 324–8
PERSSON B and STOKSTAD R G 1969 *Bull. Am. Phys. Soc.* **12** 1124
PHAN XUAN HO, BELLICARD J B, BUSSIERE A, LECONTE PH and PRIOU M *Nucl. Phys.* **A179** 529–39
POL YU S 1969 *Yad. Fiz.* **10** 771–780 (English translation: 1970 *Sov. J. Nucl. Phys.* **10** 445–50)
POWERS R J 1968 *Phys. Rev.* **169** 1–30
QUITMAN D 1967 *Z. Phys.* **206** 113–30
RAINWATER J 1957 *Ann. Rev. Nuc. Sci.* **7** 1–30
RAPHAEL R and ROSEN M 1970 *Phys. Rev.* **C1** 547–60
RAVENHALL D G and YENNIE D R 1954 *Phys. Rev.* **96** 239–40
RAWITSCHER G H 1966 *Phys. Rev.* **151** 846–52
—— 1967 in *Medium Energy Nuclear Physics with Electron Linear Accelerators* ed W Bertozzi and S Kowalski (Cambridge, Mass.: MIT) pp167–80
—— 1970 *Phys. Lett.* **33B** 445–8
REBEL H, SCHWEIMER G W, SCHATZ G, SPECHT J, LÖHKEN R, HANSER G, HABS D and KLEWE-NEBENIUS H 1972 *Nucl. Phys.* **A182** 145–73
REEHAL B S and SORENSEN R A 1970 *Phys. Rev.* **C2** 819–27
—— 1971 *Nucl. Phys.* **A161** 385–400
RINKER G A JR 1971a Invited paper presented at *Muon Physics Conf., Fort Collins, Colorado September 6–10, 1971* Los Alamos preprint LA-DC13024 (Proceedings ed P Chand to be published by Dekker, New York)
—— 1971b *Phys. Rev.* **C4** 2150–64
RIPKA G 1968 in *Advances in Physics* vol 1 ed M Baranger and E Vogt (New York: Plenum Press) pp183–259
—— 1972 Talk given at *Int. Conf. on Nucl. Structure Studies using Electron Scattering and Photo-reactions, Sendai, Japan, September* 12–15 1972
RIPKA G and GILLESPIE J 1970 *Phys. Rev. Lett.* **25** 1624–5
ROSENTHAL J E and BREIT G 1932 *Phys. Rev.* **41** 459–70
SAKURAI J J 1967 *Advanced Quantum Mechanics* (Reading, Mass.: Addison-Wesley).
SCHECK F 1972 *J. Phys., Paris* **33** Colloque C5 183–93
SCHECK F and HÜFNER J 1974 in *Muon Physics* ed V W Hughes and C S Wu (New York: Academic Press)
SCHWINGER J 1949 *Phys. Rev.* **75** 898–9

SELTZER E C 1969 *Phys. Rev.* **188** 1916–9
SENS J C 1967 *High Energy Physics and Nuclear Structure, Rehovoth* (Amsterdam: North-Holland) p93
SHAO J, BASSICHIS W H and LOMON E L 1972 *Phys. Rev.* **C6** 758–63
SHAW R R, SWIFT A and ELTON L R B 1965 *Proc. Phys. Soc.* **86** 513–8
SICK I 1973 *Phys. Lett.* **44B** 62–5
SICK I, FLOCARD H and VÉNÉRONI M 1972 *Phys. Lett.* **39B** 443–6
SICK I and MCCARTHY J S 1970 *Nucl. Phys.* **A150** 631–54
SILVER J D and STACEY D N 1973 *Proc. Roy. Soc.* A **332** 139–50
SINHA B B P, PETERSON G A, SICK I and MCCARTHY J S 1971 *Phys. Lett.* **35B** 217–8
SKARDHAMAR H F 1970 *Nucl. Phys.* **A151** 154–60
SORENSON R A 1966 *Phys. Lett.* **21** 333–4
STACEY D N 1966 *Rep. Prog. Phys.* **29** 171–215
—— 1971 *J. Phys.* B **4** 969–75
STEARNS M B 1957 *Prog. Nucl. Phys.* **6** 108
STELSON P and GRODZINS L 1965 *Nucl. Data* **A1** 21–102
STEUDEL A 1952 *Z. Physik* **132** 429–45
SUNDARESAN M K and WATSON P J S 1972 *Phys. Rev. Lett.* **29** 15–8
SWIFT A and ELTON L R B 1966 *Phys. Rev. Lett.* **17** 484–7
TAYLOR B N, PARKER W H and LANGENBERG D N 1969 *Rev. Mod. Phys.* **41** 375–496
TOEPFFER C and DRECHSEL D 1970 *Phys. Rev. Lett.* **24** 1131–4
TOMLINSON W J and STROKE H H 1964 *Nucl. Phys.* **60** 614–33
ÜBERALL H 1971 *Electron Scattering from Complex Nuclei* parts A and B (New York: Academic Press)
VAN EIJK C W E and SCHUTTE F 1970 *Nucl. Phys.* **A151** 459–64
VAN NIFTRIK G J C 1969 *Nucl. Phys.* **A131** 574–600
VAN OOSTRUM K J, HOFSTADTER R, NÖLDEKE G K, YEARIAN M R, CLARK B C, HERMAN R and RAVENHALL D G 1966 *Phys. Rev. Lett.* **16** 528–31
VAUTHERIN D and VÉNÉRONI M 1967 *Phys. Lett.* **25B** 175–8
—— 1969 *Phys. Lett.* **28B** 203–6
WALL N S 1971 *Annals Phys.* **66** 790–7
WEST D 1958 *Rep. Prog. Phys.* **21** 271–311
WHEELER J A 1947 *Phys. Rev.* **71** 320–1
WILETS L 1954 *Dan. Mat. Fys. Medd.* **29** No 3
—— 1958 *Handbuch der Physik* XXXVIII/1 (Berlin: Springer-Verlag) pp96–119
WILETS L, HILL D L and FORD K W 1953 *Phys. Rev.* **91** 1488–500
WU C S 1966 *Proc. Int. Nucl. Phys. Conf., Gatlinburg, Tenn.* ed R L Becker *et al* (New York: Academic Press)
—— 1968 *Proc. Int. Symp. on the Physics of One- and Two-electron Atoms* (Amsterdam: North-Holland)
—— 1971 *Proc. IV Int. Conf. on High Energy Physics and Nucl. Structure, Dubna*
WU C S and WILETS L 1969 *Ann. Rev. Nucl. Sci.* **19** 527–606
YEBOAH-AMANKWAH D, GRODZINS L and FRANKEL R B 1967 *Phys. Rev. Lett.* **18** 791–4
YENNIE D R, RAVENHALL D G and WILSON R R 1954 *Phys. Rev.* **95** 500–12